

1 **Anti-HIV-1 HSPC-based gene therapy with safety kill switch to defend against and attack**

2 **HIV-1 infection**

3

4 Qi Guo^{1,2,5}, Keval Parikh^{1,2}, Jian Zhang^{1,2}, Alexander Brinkley^{1,2}, Grace Chen⁴, Natnicha

5 Jakramonpreeya^{1,2,6}, Anjie Zhen^{1,3}, Dong Sung An^{1,2}

6

7 ¹UCLA AIDS Institute, UCLA, Los Angeles, CA, USA, 90024

8 ²UCLA School of Nursing, UCLA, Los Angeles, CA, USA, 90095

9 ³David Geffen School of Medicine at UCLA, Los Angeles, CA, USA, 90095

10 ⁴Department of Molecular, Cell, and Developmental Biology, UCLA, Los Angeles, CA, USA,

11 90095

12 ⁵Shanghai Key Laboratory of Tumor System Regulation and Clinical Translation, Jiading

13 Branch, Renji Hospital, Shanghai Cancer Institute, Shanghai, China, 201800

14 ⁶Chakri Naruebodindra Medical Institute, Faculty of Medicine Ramathibodi Hospital, Mahidol

15 University, Samut Prakan 10540, Thailand

16

17 Correspondence should be addressed to DSA

18 Los Angeles, California, United States of America

19 615 Charles E Young Dr S, Los Angeles, CA 90095

20 (310)-206-2063

21 dan@sonnet.ucla.edu

22 **Anti-HIV-1 HSPC gene therapy with safety switch**

23

24 **Abstract**

25 Hematopoietic stem/progenitor cell (HSPC)-based anti-HIV-1 gene therapy holds
26 promise to provide life-long remission following a single treatment. Here we report a multi-
27 pronged anti-HIV-1 HSPC-based gene therapy designed to defend against and attack HIV-1
28 infection. We developed a lentiviral vector capable of co-expressing three anti-HIV-1 genes.
29 Two are designed to prevent infection, including a short-hairpin RNA (CCR5sh1005) to knock
30 down HIV-1 co-receptor CCR5 and a membrane anchored HIV-1 fusion inhibitor (C46). The
31 third gene is a CD4-based chimeric antigen receptor (CAR) designed to attack HIV-1 infected
32 cells. Our vector also includes a non-signaling truncated human epidermal growth factor receptor
33 (huEGFRt) which acts as a negative selection-based safety kill switch against transduced cells.
34 Anti-HIV-1 vector-transduced human CD34+ HSPC efficiently reconstituted multi-lineage
35 human hematopoietic cells in humanized bone marrow/liver/thymus (huBLT) mice. HIV-1 viral
36 load was significantly reduced (1-log fold reduction, $p < 0.001$) in transplanted huBLT mice.
37 Anti-huEGFR monoclonal antibody Cetuximab (CTX) administration significantly reduced
38 huEGFRt+ vector-modified cells (>4-fold reduction, $p < 0.01$) in huBLT mice. These results
39 demonstrate that our strategy is highly effective for HIV-1 inhibition, and that CTX-mediated
40 negative selection can deplete anti-HIV-1 vector-modified cells in the event of unwanted adverse
41 effects in huBLT mice.

42

43

44

45

46

47 **Introduction**

48 Forty years after its discovery, HIV-1 infection remains a significant public health issue
49 with a total of over 39 million cases and more than 1.3 million new cases globally in 2023
50 alone.¹ Although antiretroviral therapy (ART) has significantly improved life expectancy and
51 health of those living with HIV, it cannot cure HIV-1 infection.²⁻⁶ Life-long treatment is
52 necessary due to the persistence of HIV-1 infection by producing latent HIV-1 viral reservoirs.⁴⁻⁷
53 Other shortcomings of ART include patient adherence, administrative availability, drug cost, and
54 adverse side effects. Moreover, ART reduces but does not prevent all of the known
55 complications of HIV-1 infection.⁸⁻¹² A novel therapeutic approach for life-long remission
56 without ART or elimination is critical to address these issues.^{5,13}

57 Thus far, HIV-1 cure has only been achieved in a few patients who have undergone
58 hematopoietic stem cell transplantation (HSCT) from HLA type fully or partially matched
59 allogeneic CCR5 Δ 32/ Δ 32 homozygous donors.¹⁴⁻¹⁹ In these few patients, allogeneic
60 transplantation with CCR5 Δ 32/ Δ 32 HSPC to treat underlying leukemia has also led to long-term
61 HIV-1 remission without the need for ART after successful repopulation of immune cells lacking
62 the HIV-1 co-receptor CCR5. These handful HIV-1 cure cases offer great hope for the
63 development of an HSPC-based anti-HIV-1 gene therapy that provides long-term remission or
64 cure for HIV-1 infection. However, CCR5 Δ 32/ Δ 32 homozygous mutation is found in less than
65 1% of the global population.^{20,21} Furthermore, allogeneic stem cell transplantation also requires
66 HLA-matching,¹⁶⁻¹⁸ making it extremely difficult to identify a HLA type matched donor with
67 CCR5 Δ 32/ Δ 32 homozygous mutation. Despite this, HSPC-based gene therapy to genetically
68 modify autologous cells with anti-HIV-1 genes holds great promise to provide life-long

69 remission or cure following a single treatment.^{22–24} Unlike HSCT, autologous HSPC-based gene
70 therapy uses a patient’s own cells and hence does not require HLA-matching.^{23,25}
71 Anti-HIV-1 HSPC-based gene therapy may require a multi-target approach to effectively
72 inhibit HIV-1, similar to the combinatorial drug treatment strategy used in ART.^{26,27} We
73 previously identified and proved the potent antiviral activity of a non-toxic short hairpin RNA
74 against CCR5 (CCR5sh1005) to down regulate CCR5 expression by RNA interference to protect
75 cells from HIV-1 entry.^{28,29} Although our CCR5sh1005 was efficient for down regulating CCR5
76 in human CD4+ T cells and HIV-1 inhibition through HSPC gene-modification in humanized
77 BLT mice and rhesus macaques, it does not fully ablate CCR5 expression.^{30–33} We therefore
78 added a membrane anchored anti-HIV-1 fusion inhibitor C46, which targets gp41 on HIV-1
79 virions to prevent fusion into host cells, a critical viral entry step.^{30,31,33} These anti-HIV-1 genes
80 work synergistically to protect cells by inhibiting HIV-1 binding and fusion before viral
81 integration to prevent the establishment of chronic HIV-1 infection. We previously demonstrated
82 that dual anti-HIV-1 combinations (CCR5sh1005 and C46) improved HIV-1 inhibition compared
83 to CCR5sh1005 alone and inhibited both R5-tropic and X4-tropic HIV-1.³³

84 In addition to defending HSPC against HIV-1 infection by use of the aforementioned
85 anti-HIV-1 genes, we reasoned that the potential for chronic remission of HIV-1 infection could
86 be increased by simultaneously engineering a host immunological attack on HIV-1 infected cells.
87 We incorporated a CD4-based anti-HIV-1 CAR that has demonstrated robust HIV-1 viral load
88 reduction when expressed in HSPC, producing anti-HIV-1 CAR T cells to attack and eliminate
89 HIV-1 infected cells.³⁴ CD4-based anti-HIV-1 CARs are designed to bind a HIV-1 GP120
90 envelope glycoprotein on cell surface with the extracellular CD4 D1D2 HIV-1-binding domain
91 and transmit signals through the intracellular CD3- ζ signaling domain to kill HIV-1 infected cells

92 by T cell mediated cytotoxicities.^{35,36} D1D2CAR 4-1BB is a truncated version of the previously
93 used CD4CAR and includes a 4-1BB costimulatory domain shown to enhance CAR-T cell
94 function and proliferation compared to other anti-HIV-1 CAR-T cell variants *in vivo*.³⁷
95 D1D2CAR 4-1BB also does not mediate HIV-1 infection and when coupled with anti HIV-genes
96 such as CCR5sh1005 provide gene-modified cells with extra protection.³⁷ CD4-based CARs has
97 been co-expressed in dual combination lentiviral vectors with C46 or CCR5sh1005.^{34,37} We
98 hypothesize that triple-expression of CCR5sh1005, C46, and D1D2CAR 4-1BB in HSPC will
99 durably protect infection-susceptible progeny cells and target HIV-1 infected cells, thereby
100 inhibiting 3 different steps in HIV-1 infection.

101 Despite a superior safety profile in our humanized mice and NHP studies,^{34,37,38}
102 incorporating a negatively-selectable safety kill switch into our gene therapy could prove
103 important for our approach. Anti-HIV-1 CAR T vector-modified cells may potentially cause
104 unexpected health issues such as cytokine release syndrome and CAR-T cell related
105 encephalopathy syndrome in hosts, as seen in cancer immunotherapy.³⁹⁻⁴¹ To improve safety of
106 our HSPC-based anti-HIV-1 gene therapy, we incorporated a safety kill-switch by co-expressing
107 the non-functional truncated form of human epidermal growth receptor (huEGFRt), which can be
108 targeted with the clinically available chimeric immunoglobulin G1 anti-EGFR monoclonal
109 antibody (mAb), Cetuximab (CTX) (ErbixTM).^{42,43} Administration of CTX can negatively
110 select huEGFRt expressing vector-modified cells *in vivo* through antibody-dependent cellular
111 cytotoxicity (ADCC) and complement dependent cytotoxicity (CDC). To prevent off-target
112 activation of CAR T-cells while retaining a marker function for the tracking of vector-modified
113 cells via mAb staining and flow cytometry analysis, huEGFRt lacks the extracellular ligand
114 binding domains I and II and the entire cytoplasmic tail necessary for signaling in EGFR.⁴²

115 In this report, we developed a multi-pronged anti-HIV-1 lentiviral vector with a safety
116 kill switch for efficient HSPC transduction and expression of factors capable of protecting cells
117 against and attacking HIV-1 infection. We investigated the ability of our newly developed anti-
118 HIV-1 gene lentiviral vectors to genetically modify human CD34+ HSPC, and the ability to
119 transplant and engraft these vector-modified cells to inhibit HIV-1 infection *in vivo* in huBLT
120 mice. Furthermore, we investigated a safety kill switch by CTX-mediated negative selection of
121 huEGFRt+ vector-modified cells. Together, these elements work together to provide a robust and
122 safe anti-HIV-1 HSPC-based gene therapy strategy.

123

124 **Results**

125 **Development of lentiviral vectors with a safety kill switch to defend and attack HIV-1**

126 **infection**

127 We developed two new lentiviral vectors (M1 vector: MNDU-anti-HIV-1-huEGFRt and
128 U1 vector: UbC-anti-HIV-1-huEGFRt) to effectively co-express three anti-HIV-1 genes to
129 defend against and attack HIV-1 infection and to express the huEGFRt cell surface marker as a
130 safety kill switch (Figure 1A). We expressed CCR5sh1005 from a transcriptionally weaker H1
131 RNA Polymerase III promoter to avoid toxic effects of shRNA overexpression, as previously
132 described.^{28,29} We first examined a modified Moloney Murine Leukemia virus long terminal
133 repeat promoter (MNDU) and a Ubiquitin C (Ubc) RNA polymerase II promoter to optimize the
134 co-expression of D1D2CAR 4-1BB and huEGFRt expression in M1 vector and U1 vector,
135 respectively. These two transgenes were linked by a self-cleaving T2A sequence for equimolar
136 expression. C46 was expressed from a shorter version of the eukaryotic translation elongation
137 factor 1 α (EF1 α) promoter to maintain efficient expression as the last transgene inserted near

138 the 3'LTR. Despite the multiple promoters and transgenes, the titers of our newly developed
139 anti-HIV-1 vectors in 293T cells were high ($2.75 \times 10^8 \pm 3.03 \times 10^7$ IU/mL for the M1 vector and
140 $1.00 \times 10^8 \pm 1.95 \times 10^7$ IU/mL for the U1 vector) (Figure 1B), which is consistent with our
141 previously developed lentiviral vectors.³¹ Normalized % CCR5 expression was reduced to 76.1%
142 and 69.8% in M1 and U1 vector transduced huEGFRt+ MT4-CCR5 cells, respectively,
143 compared to the normalized %CCR5 in Non-CCR5sh1005 vector transduced huEGFRt+ cells
144 (100%) (Figure 1C). Mean fluorescent intensity (MFI) of CCR5 expression in huEGFRt+ cells
145 was reduced to 1491 and 1238 in M1 and U1 vector transduced huEGFRt+ cells, respectively,
146 compared to 10526 in Non-CCR5sh1005 vector transduced huEGFRt+ cells. These results show
147 CCR5 expression was efficiently down-regulated in M1 and U1 vector-transduced huEGFRt+
148 MT4-CCR5 cells. We noticed that MFI of huEGFRt expression were lower in M1 (1197) and U1
149 (1139) vector transduced cells than that of non-CCR5sh1005 vector transduced cells (5665) (Fig
150 1C), suggesting that huEGFRt expression might be compromised due to 4 multiple transgene
151 expressions from one vector. C46 was efficiently expressed in both M1 (94.6% C46+) and
152 U1(98.9% C46+) vector-transduced MT4-CCR5 cells (Figure 1D). D1D2CAR 4-1BB and
153 huEGFRt were efficiently co-expressed in vector-transduced human primary CD8+ T cells by
154 both the M1 vector (36.4%) and U1 vector (49.1%) (Figure 1E). These results show that our
155 newly developed vectors are highly efficient for co-expressing three anti-HIV-1 genes and
156 huEGFRt in human T-cell line and primary human T cells *in vitro*. Both R5-tropic HIV-1_{NFNSX-}
157 _{SL9} and X4-tropic HIV-1_{NL4-3} infection were inhibited in M1 and U1 vector transduced MT4-
158 CCR5 cell line *in vitro* (Figure 1F). To examine cell killing activity of M1 and U1 vector-
159 transduced CD8+ CAR T cells, we performed cytotoxic T lymphocyte (CTL) assays by co-
160 incubating vector-transduced CD8+ T cells with either ACH2 cells stimulated to express high

161 levels of HIV-1 envelope (Env+) or unstimulated ACH2 cells (Env-). We observed
162 approximately 60% specific killing for both M1 and U1 vector-transduced CAR T cells at an E:T
163 ratio of 5:1 ($p < 0.01$, $p < 0.05$, respectively) (Figure 1G). These results reinforce the potential of
164 D1D2CAR 4-1BB to specifically target and induce cellular cytotoxicity in HIV-1 envelope
165 expressing cells. Altogether, these results demonstrate successful construction of a multi-pronged
166 anti-HIV-1 lentiviral vector that can block both R5- and X4-tropic HIV-1 infection *in vitro* and
167 direct a cellular immune response against infected cells via a chimeric antigen receptor.

168

169 **Efficient engraftment of vector-modified HSPC for HIV-1 viral load reduction in huBLT** 170 **mice**

171 We next investigated the efficiency of vector transduction and transplantation of human
172 CD34+ HSPC to assess the engraftment, multi-lineage hematopoietic cell reconstitution,
173 transgene expression and HIV-1 inhibition *in vivo* in the huBLT mouse model (Figure 2A). M1
174 and U1 vectors efficiently transduced human fetal liver derived CD34+ HSPC (FL-CD34+
175 HSPC) at multiplicity of infection (MOI) 3 *ex vivo*. D1D2CAR 4-1BB+/huEGFRt+ co-
176 expressing cell population reached 79.9% and 51.7% in M1 and in U1 vector-transduced FL-
177 CD34+ HSPC at day 4 post vector transduction (Figure 2B). The MFI of D1D2CAR 4-1BB
178 (13080) and huEGFRt (14806) expression in the M1 vector-transduced HSPC was notably
179 higher than that of the U1 vector-transduced HSPC D1D2CAR 4-1BB (889) and huEGFRt
180 (1344), similar to the vector-transduced human primary CD8+ T cells (Figure 1E). Multi-lineage
181 colony formation in *ex vivo* culture showed similar % of multi colony-forming units between
182 untransduced, M1, and U1 vector-transduced FL-CD34+ HSPC *ex vivo* (Figure S1). After
183 transplantation of vector-transduced FL-CD34+ HSPC in huBLT mice, total CD45+, CD3+,

184 CD4⁺ and CD8⁺ T, and CD19⁺ B multilineage human hematopoietic cells were reconstituted
185 and continued to expand in peripheral blood in huBLT mice, as previously reported.^{44,45} There
186 were no significant differences between untransduced control, M1, and U1 vector-transduced
187 FL-CD34⁺ HSPC transplanted huBLT mouse groups (herein referred to as untransduced, M1,
188 U1 huBLT mice, respectively) (Figure 2C). The average vector DNA copies/human cell were
189 higher in M1 vs U1 huBLT mice (~2 copies/cell vs ~1 copy/cell) and stably maintained during
190 the experiment (Figure 2D). The higher vector copy number in M1 huBLT mice compared to U1
191 huBLT mice could be attributed to a higher packaging efficiency of a lentiviral vector with an
192 MNDU promoter, as previously reported.⁴⁶ In a subsequent experiment, similarly high vector
193 copy levels (~1.5 copies/cell) were detected in M1 huBLT mice (Figure S2). Absolute numbers
194 of huEGFRt⁺ human CD3⁺, CD4⁺ and CD8⁺ T cells, but not CD19⁺ B cells significantly
195 increased in M1 vector-modified huBLT mice compared to U1 vector-modified and
196 untransduced huBLT mice after 4 to 6-weeks post-R5 tropic HIV-1_{NFNSX-SL9} challenge in
197 peripheral blood (Figure 2E), suggesting CCR5sh1005 and C46 may provide protection for M1
198 vector-modified human CD4⁺ T cells for selective growth advantage, and D1D2CAR 4-1BB
199 may provide a CAR-dependent proliferation advantage. Percentage of huEGFRt⁺ cells did not
200 show increase in peripheral blood in M1 huBLT mice and in U1 huBLT mice because huEGFRt⁻
201 cells also increased in the huBLT mice (Figure S3, S4, and S5) as total human hematopoietic
202 cells continue to increase in huBLT mice (Figure 2C).

203 To examine if vector-modified cells from the huBLT mice could respond to HIV-1
204 envelope protein, we performed *ex vivo* cytokine release assays using HIV-1 Env⁺ ACH2 cells
205 as targets. When mixed with HIV-1 Env⁺ ACH2 cells, human CD8⁺ splenocytes from M1
206 huBLT mice exhibited significantly higher IFN- γ expression compared to CD8⁺ splenocytes

207 from M1 huBLT mice mixed with HIV-1 Env- ACH2 cells (~3 fold increase, $p < 0.05$) and CD8+
208 splenocytes from control untransduced huBLT mice mixed with HIV-1 Env+ ACH2 cells (~5
209 fold increase, $p < 0.05$) consistent with an HIV-1 envelope-specific cytokine response (Figure 2F,
210 Figure S6). The HIV-1 plasma viral load was significantly reduced ($p < 0.001$, 1-log reduction)
211 for 6 weeks post HIV-1 challenge in M1 huBLT mice compared to untransduced huBLT mice,
212 which served as our negative control. We also observed reduction of HIV-1 viral load for up to 4
213 weeks post HIV-1 challenge in U1 huBLT mice (~4 fold reduction, $p < 0.05$), but viral load
214 reduction was not significant at 6 weeks post infection. Because the M1 vector showed more
215 significant viral load reduction in our donor 1 experiment, we further investigated the M1 vector
216 and validated the effectiveness of HIV-1 viral load reduction in M1 huBLT mice in a repeat
217 experiment with donor 2 (~1 log-fold reduction, $p < 0.05$) (Figure 2G). These results demonstrate
218 that our multi-pronged anti-HIV-1 HSPC-based gene therapy strategy with M1 vector can
219 achieve efficient *ex vivo* CD34+ cell transduction, support multi-lineage human hematopoietic
220 cell reconstitution, stable transgene expression and greater viral load reduction compared to the
221 U1 vector in huBLT mice.

222

223 **CTX-mediated negative selection of huEGFRt+ vector-modified cells as a safety kill switch**

224 Although adverse effects have not been reported in anti-HIV-1 HSPC-based gene therapy
225 preclinical studies or in clinical trials, potential adverse side-effects from lentiviral vector
226 transduced HSPC or the induction of anti-HIV-1 CAR T cells must be approached prospectively.
227 We therefore incorporated a safety kill switch into our anti-HIV-1 gene lentiviral vector,
228 huEGFRt, triggered by the cognate CTX antibody. We investigated CTX-mediated negative
229 selection of huEGFRt+ vector-modified cells in huBLT mice (Figure 3A). In our first

230 experiment, we observed transient reduction of huEGFRt+ vector-modified cells in M1 huBLT
231 mice (Figure S7). Since reconstituted human immune function in humanized mouse models is
232 suboptimal, we hypothesized that our initial modest results were due to the limited number of
233 human NK cells in huBLT mice.^{47,48} To enhance the number of functional human NK cells for
234 ADCC, we injected human NK cells and an IL-15 expressing lentiviral vector to promote
235 survival and function of human NK cells. In this augmented humanized mouse model, the
236 percentage and absolute cell number of huEGFRt+ M1 vector-modified cells were significantly
237 reduced following CTX treatment. We observed substantial reductions in CD45+, CD3+, CD4+,
238 CD8+, and CD4+/CD8+ multi-lineage hematopoietic cells in peripheral blood of CTX-treated
239 animals compared to CTX-untreated mice after 1 week of CTX injections; this difference
240 persisted for 4 weeks (~13 fold reduction, $p < 0.01$, and ~13 fold reduction, $p < 0.05$,
241 respectively, averaged across all cell lineages at week 4 post-CTX treatment) (Figure 3B and
242 3C). HuBLT mice were euthanized at 4 weeks post CTX injections; huEGFRt+ vector-modified
243 cells were significantly reduced in spleen and BM (~ 9 fold reduction, $p < 0.01$, and ~ 2.5 fold
244 reduction, $p < 0.01$, respectively, averaged across all cell lineages at week 4 post-CTX treatment)
245 in CTX-treated vs CTX-untreated control M1 huBLT mice (Figure 3D, Figure S8). Within
246 HSPC population, huEGFRt+ vector-modified CD34+/CD90+/CD38- HSPC were likewise
247 significantly reduced (~3 fold reduction $p < 0.05$) in the BM of CTX-treated M1 huBLT mice
248 ($2.12\% \pm 1.20\%$) compared to CTX-untreated M1 huBLT mice ($21.67\% \pm 7.92\%$) (Figure 3E
249 and 3F). HuBLT mice remained healthy in CTX-treated and untreated groups, suggesting no
250 apparent health adverse effects (Figure S9).

251 Finally, we utilized Phycoerythrin (PE) conjugated CTX (CTX-PE) to stain huEGFRt+
252 cells and to analyze the level of expression by flow cytometry. To test whether CTX-mediated

253 negative selection could impede detection of huEGFRt⁺ cells with the same antibody, we
254 compared CTX-PE to another anti-huEGFR PE-conjugated mAb, Matuzumab (MTZ-PE), which
255 binds to a different epitope on huEGFR (Figure S10).⁴⁹ MTZ-PE staining confirmed that CTX-
256 treated huEGFRt⁺ splenocytes from M1 huBLT mice were significantly reduced in multiple cell
257 lineages (CD45⁺, CD3⁺, CD4⁺, CD8⁺) compared to CTX-untreated splenocytes from M1
258 huBLT mice (~13-fold reduction, p <0.01 averaged across all cell lineages) (Figure S11). The
259 lower %huEGFRt expression estimated by MTZ-PE staining may reflect the lower binding
260 affinity of MTZ-PE than CTX-PE. Despite this difference, both MTZ-PE and CTX-PE stained
261 CTX-treated M1 huBLT mice splenocytes showed significant reductions in huEGFRt
262 expression. These results demonstrate that our CTX-mediated negative selection strategy is
263 highly effective for depleting huEGFRt⁺ vector-modified human HSPC and progeny cells for
264 diverse cell and gene therapies in huBLT mice.

265

266 **Discussion**

267 In this study, we investigated a multi-pronged anti-HIV-1 HSPC based gene strategy to
268 defend against and attack HIV-1 infection in humanized BLT mice. We developed a novel
269 lentiviral vector that successfully co-expressed three anti-HIV-1 genes. These anti-HIV-1 genes
270 include an shRNA against CCR5 HIV-1 co-receptor and C46 fusion inhibitor to protect cells
271 against HIV-1 infection, and a truncated CD4-based CAR with 4-1BB costimulatory domain
272 (D1D2CAR 4-1BB) to attack HIV-1 infected cells. We also incorporated huEGFRt, to allow for
273 efficient negative selection of vector-modified cells as a safety kill switch in case of potential
274 adverse effects. Our results demonstrate that vector-modified HSPC efficiently reconstituted
275 anti-HIV-1 vector-modified cells and significantly reduced viral load *in vivo* in huBLT mice. We

276 used huBLT mice since the development of human HSPC derived anti HIV-1 gene modified T
277 cells occurs in the donor matched human thymus tissue. In other humanized mouse models,
278 human T cell development occurs in mouse thymus and it is not efficient nor physiological due
279 to the human leukocyte antigen (HLA) and mouse MHC mismatch.^{44,50,51} Administration of
280 CTX, a clinically available anti-huEGFR monoclonal antibody, significantly reduced huEGFRt+
281 gene-modified cells, improving the safety of our anti-HIV-1 gene therapy strategy.

282 HSPC-based gene therapy has been investigated to achieve life-long remission or cure
283 due to the potential of anti-HIV-1 gene modified HSPC to continuously provide HIV-1 protected
284 immune cells.²²⁻²⁴ Unfortunately, the efficiency of gene modification in HSPC and the level of
285 engraftment are not sufficient to achieve life-long remission with current technologies.²²⁻²⁵ If the
286 engraftment and reconstitution is incomplete, remaining unprotected cells are subject to
287 infection. CAR T-cells have emerged as a powerful immunotherapy for different forms of
288 cancer.^{52,53} Anti-HIV-1 CAR gene can re-engineer host immune cells to target HIV-1 specific
289 antigens such as gp120 on the surface of HIV-1 infected cells and elicit virus-specific
290 cytotoxicity.^{37,54,55} This strategy subverts the necessity for complete engraftment of anti-HIV-1
291 vector modified HSPC, as anti-HIV-1 CAR T cells can attack HIV-1 infected cells. In addition to
292 CCR5sh1005 and C46, we successfully developed a lentiviral vector capable of co-expressing a
293 CD4-based D1D2CAR 4-1BB for efficient HSPC gene modification to achieve efficient viral
294 load reduction.

295 We successfully incorporated a safety kill switch by co-expressing huEGFRt in our anti-
296 HIV-1 HSPC based gene strategy to better prepare for potential adverse effects such as clonal
297 outgrowth or malignant transformation of lentiviral vector transduced HSPC by random vector
298 insertional mutagenesis, CAR T cell mediated cytokine release syndrome, or encephalopathy

299 syndrome.^{34,38,40,56-58} We chose huEGFRt cell surface marker gene due to its relatively short
300 cDNA sequence, allowing for its inclusion and efficient co-expression in a complex multi-
301 pronged lentiviral vector. HuEGRt can be targeted with the clinically available chimeric
302 immunoglobulin G1 anti-EGFR monoclonal antibody (mAb), Cetuximab (CTX) (ErbixTM) for
303 efficient negative selection.^{42,43} Furthermore, huEGFRt expression can be monitored by
304 fluorescence conjugated anti-huEGFR mAb and flow cytometry, giving it a secondary purpose
305 as a trackable gene marker of vector modified cells.⁴²

306 Other negative selection strategies of vector-modified HSPC have been developed using
307 CD20 paired with rituximab, herpes simplex virus-thymidine kinase (HSV-TK) paired with
308 ganciclovir, and inducible caspase 9 (iCas9) paired with AP1903 (Rimiducid) to induce
309 dimerization.⁵⁹⁻⁶¹ CTX-mediated negative selection of huEGFRt+ cells stands out as a promising
310 safety switch for several compelling reasons. Unlike rituximab used to deplete CD20+ cells,
311 CTX has not been shown to cause late onset neutropenia in clinical trials.^{42,43,62,63} CTX-mediated
312 elimination of huEGFRt+ cells also holds several advantages to the HSV-TK system. The HSV-
313 TK system paired with ganciclovir is only functional on proliferating cells, and a loss of
314 sensitivity of ganciclovir could further stifle this method's effectiveness.^{64,65} Studies have also
315 indicated the potential for immunogenicity against HSV-TK, and its interference with host DNA
316 repair, greatly enhancing the potential for unwanted cytotoxicity.^{66,67} The iCas9 system has
317 shown promise, with exposure to AP1903 leading to elimination of 85-95% of circulating iCas9-
318 transduced cells *in vitro* and *in vivo*.⁶⁸⁻⁷⁰ However, there are limitations to the iCas9 system's
319 practical application in clinical trials, as safety switches derived from non-human sequences will
320 likely increase the risk of immunogenicity.⁷¹⁻⁷³ The significant reduction of huEGFRt+ vector-

321 modified cells by CTX in huBLT mice in this study combined with prior use in clinical studies
322 suggests its efficacy as a safe and successful kill-switch system for HSPC-based gene therapies.

323 In summary, we provided a proof of concept that our newly developed multi-pronged
324 anti-HIV-1 gene lentiviral vector with a safety kill switch could mediate efficient HSPC CD34+
325 transduction, engraftment, viral load reduction, and negative selection of vector modified cells *in*
326 *vivo* in huBLT mice. Our studies performed in humanized BLT mice provide valuable insight on
327 the development, protection, and efficacy of engineered T cells from anti-HIV-1 gene modified
328 human HSPC developed through the human thymus. For clinical application, we recognize that
329 there are still many obstacles to overcome. Further investigation of our strategies in more
330 clinically relevant animal models, such as non-human primates, could provide us more clinically
331 relevant results. We believe continuous improvements in the level of HIV-1 inhibition by
332 enhancing the engraftment of anti-HIV-1 gene modified HSPC and ensuring safety will
333 ultimately succeed us to translate our HSPC based anti-HIV-1 gene therapy into clinic.

334

335 **Materials and Methods**

336 This study was carried out in strict accordance with the recommendations in the Guide
337 for the Care and Use of Laboratory Animals of the National Institutes of Health (“The Guide”),
338 and was approved by the Institutional Animal Care and Use Committees of the University of
339 California, Los Angeles, protocol #ARC-2007-092. For humanized mice, all surgeries were
340 performed under ketamine/xylazine and isoflurane anesthesia, and all efforts were made to
341 minimize animal pain and discomfort.

342

343 **Vector Construction**

344 Our vector construct backbone is derived from the “EQ” plasmid (generously provided
345 by Satiro N. De Oliveira, UCLA, Los Angeles, California).⁴³ We inserted our previously
346 constructed CCR5sh1005,²⁹ D1D2CAR 4-1BB previously published by Zhen et al,³⁷ and also
347 the membrane anchored HIV-1 fusion inhibitor C46 previously published by Burke et al.³⁰ Final
348 optimized constructs also included the CD8 stalk element after the D1D2CAR 4-1BB
349 extracellular domains and before the CD8 transmembrane domain in the D1D2CAR 4-1BB.
350 Ubiquitin C or modified MLV long terminal repeat (MNDU3) promoters were used in each
351 vector respectively to express D1D2CAR 4-1BB and huEGFRt. C46 was expressed using a
352 truncated elongation factor-1a (EF1a) promoter. The final construct plasmids (M1 and U1) were
353 purified using QIAquick Gel Extraction Kit (Qiagen, Hilden, Germany). Stellar competent cells
354 from Takara Bio (Kusatsu, Shiga, Japan) were transformed with our constructed plasmids, and
355 plasmid stocks were then produced using Macherey-Nagel Nucleobond Xtra Midi Kit
356 (Macherey-Nagel, Düren, Germany).

357

358 **Cell culture**

359 MT4-CCR5 cells are a human T-lymphotropic virus type 1-transformed human CD4⁺ T
360 cell line that stably expresses CCR5, and were kindly provided by Dr. Koki Morizono (UCLA,
361 Los Angeles). MT4-CCR5 cells were generated by transducing MT4 cells with a lentiviral vector
362 expressing human CCR5 under the control of the internal SFFV promoter. These cells were
363 cultured in RPMI-1640 (Life Technologies, Carlsbad, CA) supplemented with 10% fetal bovine
364 serum (FBS), 2mM L-glutamine, 100 units/ml penicillin, and 100 µg/ml streptomycin (GPS).
365 Human primary peripheral blood mononuclear cells (PBMC) were isolated from whole blood
366 from healthy donors obtained by the UCLA CFAR Virology Core Laboratory using Ficoll Paque

367 Plus (GE Healthcare, Uppsala, Sweden). PBMC were cultured in RPMI-1640 supplemented with
368 20% FBS and GPS (20F RPMI). Primary human fetal liver derived (FL) CD34⁺ HSPC were
369 isolated from human fetal liver obtained from the UCLA CFAR Gene and Cellular Therapy Core
370 Laboratory (Los Angeles, California) or Advanced BioScience Resources, Inc (Alameda, CA)
371 using a CD34⁺ microbead isolation kit (Miltenyi Biotec, Auburn, CA).

372

373 **Lentivirus Production**

374 Lentiviral vectors were packaged with a VSV-G pseudotype using calcium phosphate
375 transfection, then collected from transfected HEK293T-cells treated with chloroquine and
376 concentrated in 1xHBSS via ultracentrifugation, as previously described.⁷⁴⁻⁷⁶ Titers for lentiviral
377 vectors were determined using CTX-PE mAb staining and flow cytometry in vector-transduced
378 HEK293T-cells and were based on huEGFRt expression at Day 3 post-transduction.

379

380 ***In-Vitro* HIV-1 inhibition assays**

381 We established our vectors' proof of concept to inhibit HIV-1 and target HIV-1 infection
382 *in-vitro* in cell lines and primary cells prior to *in-vivo* experiments. For our HIV Inhibition assay,
383 MT4-CCR5 cells were transduced with triple-anti-HIV vectors at MOI 1 and infected with R5-
384 tropic HIV-1_{NFNSX} virus (MOI 1) or X4-tropic HIV-1_{NL4-3} virus (MOI 0.005) at 4 days post-
385 transduction. Supernatants collected 7 days post-challenge were analyzed for p24 using Abcam
386 HIV p24 ELISA kit (Abcam, Waltham, MA). To functionally qualify D1D2CAR 4-1BB, CD8⁺
387 T cells were isolated from healthy-PBMCs provided by UCLA CFAR virology core and
388 expanded in RPMI 1640 (Gibco) with 10% fetal bovine serum (HyClone) containing IL7

389 (10ng/mL) and IL15 (5ng/mL). Cells were transduced with lentiviral vectors at MOI 3 and co-
390 cultured with either unstimulated ACH2 cells or ACH2 cells stimulated overnight with
391 PMA/Ionomycin (Invitrogen, Darmstadt, Germany) to increase HIV-1 gp120 surface protein.^{77,78}
392 ACH2 cells are a cell line with a single integrated copy of HIV-1 strain LAI. Unstimulated and
393 stimulated ACH2 cells were labeled with CellTrace™ Far Red (Invitrogen) before 16-hr co-
394 culture followed by stain with Zombie (Aqua or Green) Fixable Viability (Biolegend, San Diego,
395 CA) and KC57 antibody (Beckman Coulter, Indianapolis, IN) to detect Gag+ ACH2 cells.
396 Specific killing was calculated as follows: % specific killing = (%live Gag+ ACH2 cells co-
397 cultured with untransduced cell—%live Gag+ ACH2 cells co-cultured with vector-transduced
398 cells)/ %live Gag+ ACH2 co-cultured with untransduced cell × % Gag+ in ACH2 cells alone.

399

400 **Lentiviral Vector Transduction of HSPC for *in vivo* experiments**

401 Fetal liver-derived CD34+ HSPCs were resuspended in Yssel's medium (Gemini Bio
402 Products) with 2% BSA (Sigma-Aldrich) and seeded into 20 µg/mL RetroNectin (Clontech
403 Laboratories)-coated plates. After 1 hour of incubation at 37°C, cells were transduced with
404 lentiviral vectors at MOI 3 and cultured overnight at 37°C. The following day, vector-transduced
405 CD34+ HSPCs were transplanted into NSG mice. An aliquot of the transduced CD34+ HSPCs
406 were cultured in 10F RPMI, supplemented with cytokine stimulations (SCF, Flt-3, TPO;
407 PeproTech) at a concentration of 50 ng/mL for 3 days. The efficiencies of vector transduction
408 were evaluated by flow cytometry (Fortessa flow cytometers, BD Biosciences) and/or by vector
409 copy number (VCN) using digital PCR as described below (ThermoFisher QuantStudio 3D
410 Digital System/Quantstudio Absolute Q Digital PCR system).

411

412 **Humanized BLT Mouse Construction**

413 NSG (NOD/SCID/IL2ry ^{-/-}) mice were used to generate humanized BLT mice and
414 housed according to UCLA Humanized Mouse Core Laboratory procedures as previously
415 described.³¹ Human fetal thymus and fetal liver were obtained from Advanced Bioscience
416 Resources (ABR). Fetal tissues were obtained without patient identifying information. Written
417 informed consent was obtained from patients for the use of tissues for research purposes. Briefly,
418 one day before transplant, CD34⁺ cells were isolated from fetal livers using anti-CD34⁺
419 magnetic bead-conjugated monoclonal antibodies (Miltenyi Biotec) and transduced with vectors
420 described above. NSG mice were conditioned with sub-lethal body irradiation (270 cGy Cesium-
421 137). On the day of transplant, an equal mixture of non-transduced or vector-transduced FL-
422 CD34⁺ cells (~ 0.5x10⁶ per mouse) and CD34⁻ cells (~4.5 x10⁶ per mouse) were mixed with
423 5μL of Matrigel (BD Biosciences) and implanted with a piece of thymus under the kidney
424 capsule. Mice were then injected with non-transduced or vector-transduced CD34⁺ HSPCs (~
425 0.5x10⁶ per mouse) using a 27-gauge needle through the retro-orbital vein plexus. At 8–10 weeks
426 post-transplantation, blood was obtained from each mouse by retro-orbital sampling and
427 peripheral blood mononuclear cells were analyzed by flow cytometry to quantify human immune
428 cell engraftment.

429

430 **Colony-forming unit (CFU) assays**

431 Colony-forming units were assayed by culturing transduced and non-transduced FL-
432 CD34⁺ cells 3 days after transduction in triplicate in a 6 well plate (ThermoFisher) using
433 complete methylcellulose (MethoCult H4435 Enriched, Stem Cell Technologies). 14 days later,
434 colony-forming units (CFU) in each well were then counted by light microscopy, and the colony

435 type was scored based on morphology. Proportions of differentiated hematopoietic colonies =
436 $100\% \times (\text{each colony type CFU counted}/\text{total CFU counted})$ and calculated from each well from
437 triplicates.⁷⁹ Total CFU counts ranged from 30-75 in each well.

438

439 **HIV-1 Infection and viral load analysis**

440 NSG huBLT mice were injected with R5 tropic HIV-1_{NFNSX-SL9} (MOI 5) (200 ng p24)
441 retro-orbitally 11 weeks post-vector-modified HSPC transplant⁷⁴. Mice were bled retro-orbitally
442 every 2 weeks after infection, and blood samples were analyzed for HIV-1 viral load via RT-
443 PCR. HPSC engraftment was assessed by vector copy number assay via digital PCR, and cell
444 lineage differentiation and transgene expression were measured via flow cytometry.

445

446 **Depletion of huEGFRt+ transduced cells via Cetuximab**

447 At week 13-14 post-transplantation of vector-modified HSPC, mice were separated into
448 two groups with one group to receive CTX treatment (CTX+) alongside human NK cells and
449 huIL-15 treatment (n=5) and the other group to be left untreated (n=4). Vector-modified
450 huEGFRt+ HSPC transplanted huBLT mice were treated with cetuximab (ErbirtuxTM) at a
451 concentration of 1mg per mouse intraperitoneally for 11 consecutive days. Because of the lack of
452 efficient development of human NK cells in NSG mice, which was hypothesized to be the result
453 of a lack of IL15,⁸⁰ and to facilitate antibody dependent cellular toxicity, we injected a dose of
454 5×10^6 human NK cells isolated from healthy PBMCs one day before the first CTX treatment and
455 a second dose of 5×10^6 human NK cells from the same donor on day 7 of CTX treatment.
456 Lentiviral vectors expressing IL-15 (2.5×10^5 IU/mouse) were injected retro-orbitally on day 7 of
457 CTX treatment. huEGFRt expression and absolute cell count were monitored in multi-human

458 cell lineages by staining peripheral blood cells with CD45-, CD3-, CD19-, CD4-, and CD8-
459 specific monoclonal antibodies of peripheral blood prior to flow cytometry analysis at 3 weeks
460 before CTX treatment and 1 and 4 weeks post-CTX treatment. We developed this strategy to
461 augment negative selection results in animals lacking circulating NK cells and supportive IL-15,
462 as NK cells serve a critical role in CTX-mediated ADCC of huEGFRt+ cells (**Figure S7**).

463

464 **Analysis of tissue from transduced huBLT mice**

465 Humanized BLT mice were sacrificed at week 18-19 post-transplant, and the spleen and
466 BM tissues were harvested. Tissue samples were collected in MACS tissue storage solution
467 (Miltenyi Biotec, 130-100-008) at necropsy and processed immediately for single cell isolation
468 as described previously.^{31,37} Isolated cells were stained for surface markers and analyzed by flow
469 cytometry or vector copy number was determined by digital PCR.

470 Single-cell suspensions prepared from peripheral blood, spleen, or BM of huBLT mice
471 were stained for surface markers and acquired on a LSRFortessa flow cytometer (BD
472 Biosciences). The following antibodies were used: CD45-eFluor 450 (HI30, eBioscience), CD3-
473 APC H7 (SK7, Pharmingen), CD4-APC (OKT4, eBioscience), CD8-PerCP Cy5.5 (SK1,
474 BioLegend), CD19-Brilliant Violet 605 (HIB19, BD Horizon), EGFR-PE (Hu1, R&D Systems),
475 and Countbright beads (Invitrogen). Red blood cells were lysed with RBC Lysis Buffer
476 (Biolegend) after cell surface marker staining. Stained cells were fixed with 2% formaldehyde in
477 PBS. The data were analyzed by FlowJo v.10 (Tree Star) software.

478

479 **Determination of vector copy number (VCN)**

480 Cell pellets from 25 μ L peripheral blood, spleen, or BM of huBLT mice were lysed with
481 5 μ L of 0.2M NaOH in a 75 \square water bath for 5 min. Cell lysates were cooled in a 4 $^{\circ}$ C refrigerator
482 for 5 min. 45 μ L Tri-HCl was added to neutralize the lysates. The lysate cells were directly used
483 in dPCR set at 96 $^{\circ}$ C for 10 min, followed by 42 cycles of denaturation at 98 $^{\circ}$ C for 15 s,
484 annealing at 60 $^{\circ}$ C for 2 min, and a final extension at 60 $^{\circ}$ C for 2 min. The primers and probe
485 specific to WPRE were customized by ThermoFisher, which are primer sequence 1, 5' -
486 CCTTTCCGGGACTTTCGCTTT-3', primer sequence 2, 5'-GCAGGCGGCGATGAGT-3', and
487 probe 5'-(FAM)-CCCCCTCCCTATTGCC-3'. The primers and probe specific to β -globin were
488 purchased from ThermoFisher (cat#4448489). Average VCN was determined by multiplex
489 dPCR of the WPRE sequence in the vector and normalized to the cell housekeeper gene β -
490 globin.

491

492 **Statistical Analysis**

493 Statistical analysis was performed using software Prism. Mann-Whitney U test was used
494 for nonparametric testing of independent groups, and student's t-test were used for parametric
495 testing of independent groups. Statistical significance was evaluated as *p <0.05. Other
496 significance levels are indicated as follows: **p <0.01, ***p <0.001, and ****p <0.0001.

497

498 **Data Availability Statement**

499 The data supporting the findings of this study are available from the corresponding author upon
500 reasonable request.

501

502 **Author contributions**

503 Authors QG, KP, and JZ contributed equally to this manuscript and are all considered co-first
504 authors. Authors AB, NJ, and GC contributed to experimental data collection and manuscript
505 revision. Authors AZ and DSA gave invaluable guidance and feedback throughout the
506 preparation of this manuscript. All authors had the opportunity to review the manuscript prior to
507 submission.

508

509 **Acknowledgements**

510 We would like to thank Sarah Schroeder, Christina Zakarian, Martin Zakarian, Kory Hamane,
511 and Dr. Scott Kitchen, Valerie Rezek and staff at UCLA Humanized Mouse & Gene Therapy
512 Core for their technical support. We would also like to thank Dr. Chris Peterson, Dr. Paul
513 Krogstad, and Dr. Irvin Chen for their feedback and revisions on drafted versions of manuscript.
514 This research was supported by the NIAID 1U19 AI149504, the UCLA-CDU Center for AIDS
515 Research NIH/NIAID AI152501, the NIAID R01AI172727 to AZ, the NIDA R01DA-52841 to
516 AZ, the amfAR 110304-71-RKRL and 110395-72-RPRL to AZ, the James B. Pendleton
517 Charitable Trust, and UCLA AIDS institute. The vector maps and experimental design figures
518 were created with biorender.com.

519

520 **Declaration of Interests**

521 DSA has a financial interest in CSL Behring. No funding was provided by the company to
522 support this work. DSA holds a US patent for CCR5sh1005. All of the other authors declare no
523 competing interests.

524

525 **Key words**

526 Hematopoietic stem/progenitor cell (HSPC) based gene therapy, HIV-1, CCR5 short-hairpin
527 RNA, CD4-based anti-HIV-1 chimeric antigen receptor, C46 membrane anchored HIV-1 fusion
528 inhibitor, truncated human EGFR (huEGFRt), Cetuximab-mediated *in vivo* negative selection,
529 humanized mouse

530

531

532 **References**

- 533 1. HIV and AIDS <https://www.who.int/news-room/fact-sheets/detail/hiv-aids>.
- 534 2. Palella, F.J., Delaney, K.M., Moorman, A.C., Loveless, M.O., Fuhrer, J., Satten, G.A.,
535 Aschman, D.J., and Holmberg, S.D. (1998). Declining morbidity and mortality among
536 patients with advanced human immunodeficiency virus infection. HIV Outpatient Study
537 Investigators. *N. Engl. J. Med.* 338, 853–860.
538 <https://doi.org/10.1056/NEJM199803263381301>.
- 539 3. Bozzi, G., Simonetti, F.R., Watters, S.A., Anderson, E.M., Gouzoulis, M., Kearney, M.F.,
540 Rote, P., Lange, C., Shao, W., Gorelick, R., et al. (2019). No evidence of ongoing HIV
541 replication or compartmentalization in tissues during combination antiretroviral therapy:
542 Implications for HIV eradication. *Sci. Adv.* 5, eaav2045.
543 <https://doi.org/10.1126/sciadv.aav2045>.
- 544 4. Lau, C.-Y., Adan, M.A., and Maldarelli, F. (2021). Why the HIV Reservoir Never Runs Dry:
545 Clonal Expansion and the Characteristics of HIV-Infected Cells Challenge Strategies to Cure
546 and Control HIV Infection. *Viruses* 13, 2512. <https://doi.org/10.3390/v13122512>.
- 547 5. Jiang, C., Lian, X., Gao, C., Sun, X., Einkauf, K.B., Chevalier, J.M., Chen, S.M.Y., Hua, S.,

- 548 Rhee, B., Chang, K., et al. (2020). Distinct viral reservoirs in individuals with spontaneous
549 control of HIV-1. *Nature* 585, 261–267. <https://doi.org/10.1038/s41586-020-2651-8>.
- 550 6. Lewin, S.R., and Rasmussen, T.A. (2020). Kick and kill for HIV latency. *Lancet Lond. Engl.*
551 395, 844–846. [https://doi.org/10.1016/S0140-6736\(20\)30264-6](https://doi.org/10.1016/S0140-6736(20)30264-6).
- 552 7. Chun, T.W., Davey, R.T., Engel, D., Lane, H.C., and Fauci, A.S. (1999). Re-emergence of
553 HIV after stopping therapy. *Nature* 401, 874–875. <https://doi.org/10.1038/44755>.
- 554 8. Chawla, A., Wang, C., Patton, C., Murray, M., Puneekar, Y., de Ruiter, A., and Steinhart, C.
555 (2018). A Review of Long-Term Toxicity of Antiretroviral Treatment Regimens and
556 Implications for an Aging Population. *Infect. Dis. Ther.* 7, 183–195.
557 <https://doi.org/10.1007/s40121-018-0201-6>.
- 558 9. Butler, K., Anderson, S.-J., Hayward, O., Jacob, I., Puneekar, Y.S., Evitt, L.A., and Oglesby,
559 A. (2021). Cost-effectiveness and budget impact of dolutegravir/lamivudine for treatment of
560 human immunodeficiency virus (HIV-1) infection in the United States. *J. Manag. Care Spec.*
561 *Pharm.* 27, 891–903. <https://doi.org/10.18553/jmcp.2021.27.7.891>.
- 562 10. Christodoulou, J., Abdalian, S.E., Jones, A.S.K., Christodoulou, G., Pentoney, S.L., and
563 Rotheram-Borus, M.J. (2020). Crystal Clear with Active Visualization: Understanding
564 Medication Adherence Among Youth Living with HIV. *AIDS Behav.* 24, 1207–1211.
565 <https://doi.org/10.1007/s10461-019-02721-3>.
- 566 11. Imahashi, M., Ode, H., Kobayashi, A., Nemoto, M., Matsuda, M., Hashiba, C., Hamano, A.,
567 Nakata, Y., Mori, M., Seko, K., et al. (2021). Impact of long-term antiretroviral therapy on
568 gut and oral microbiotas in HIV-1-infected patients. *Sci. Rep.* 11, 960.
569 <https://doi.org/10.1038/s41598-020-80247-8>.
- 570 12. Yuan, N.Y., and Kaul, M. (2021). Beneficial and Adverse Effects of cART Affect

- 571 Neurocognitive Function in HIV-1 Infection: Balancing Viral Suppression against Neuronal
572 Stress and Injury. *J. Neuroimmune Pharmacol. Off. J. Soc. NeuroImmune Pharmacol.* *16*,
573 90–112. <https://doi.org/10.1007/s11481-019-09868-9>.
- 574 13. Blazkova, J., Gao, F., Marichannegowda, M.H., Justement, J.S., Shi, V., Whitehead, E.J.,
575 Schneck, R.F., Huiting, E.D., Gittens, K., Cottrell, M., et al. (2021). Distinct mechanisms of
576 long-term virologic control in two HIV-infected individuals after treatment interruption of
577 anti-retroviral therapy. *Nat. Med.* *27*, 1893–1898. [https://doi.org/10.1038/s41591-021-](https://doi.org/10.1038/s41591-021-01503-6)
578 01503-6.
- 579 14. Allers, K., Hütter, G., Hofmann, J., Loddenkemper, C., Rieger, K., Thiel, E., and Schneider,
580 T. (2011). Evidence for the cure of HIV infection by CCR5 Δ 32/ Δ 32 stem cell
581 transplantation. *Blood* *117*, 2791–2799. <https://doi.org/10.1182/blood-2010-09-309591>.
- 582 15. Hütter, G., Nowak, D., Mossner, M., Ganepola, S., Müssig, A., Allers, K., Schneider, T.,
583 Hofmann, J., Kücherer, C., Blau, O., et al. (2009). Long-term control of HIV by CCR5
584 Delta32/Delta32 stem-cell transplantation. *N. Engl. J. Med.* *360*, 692–698.
585 <https://doi.org/10.1056/NEJMoa0802905>.
- 586 16. Gupta, R.K., Abdul-Jawad, S., McCoy, L.E., Mok, H.P., Peppas, D., Salgado, M., Martinez-
587 Picado, J., Nijhuis, M., Wensing, A.M.J., Lee, H., et al. (2019). HIV-1 remission following
588 CCR5 Δ 32/ Δ 32 haematopoietic stem-cell transplantation. *Nature* *568*, 244–248.
589 <https://doi.org/10.1038/s41586-019-1027-4>.
- 590 17. Hsu, J., Van Besien, K., Glesby, M.J., Pahwa, S., Coletti, A., Warshaw, M.G., Petz, L.,
591 Moore, T.B., Chen, Y.H., Pallikkuth, S., et al. (2023). HIV-1 remission and possible cure in
592 a woman after haplo-cord blood transplant. *Cell* *186*, 1115-1126.e8.
593 <https://doi.org/10.1016/j.cell.2023.02.030>.

- 594 18. Jensen, B.-E.O., Knops, E., Cords, L., Lübke, N., Salgado, M., Busman-Sahay, K., Estes,
595 J.D., Huyveneers, L.E.P., Perdomo-Celis, F., Wittner, M., et al. (2023). In-depth virological
596 and immunological characterization of HIV-1 cure after CCR5 Δ 32/ Δ 32 allogeneic
597 hematopoietic stem cell transplantation. *Nat. Med.* 29, 583–587.
598 <https://doi.org/10.1038/s41591-023-02213-x>.
- 599 19. HIV-1 cure after CCR5 Δ 32/ Δ 32 allogeneic hematopoietic stem cell transplantation (2023).
600 *Nat. Med.* 29, 547–548. <https://doi.org/10.1038/s41591-023-02215-9>.
- 601 20. Solloch, U.V., Lang, K., Lange, V., Böhme, I., Schmidt, A.H., and Sauter, J. (2017).
602 Frequencies of gene variant CCR5- Δ 32 in 87 countries based on next-generation sequencing
603 of 1.3 million individuals sampled from 3 national DKMS donor centers. *Hum. Immunol.* 78,
604 710–717. <https://doi.org/10.1016/j.humimm.2017.10.001>.
- 605 21. Huang, Y., Paxton, W.A., Wolinsky, S.M., Neumann, A.U., Zhang, L., He, T., Kang, S.,
606 Ceradini, D., Jin, Z., Yazdanbakhsh, K., et al. (1996). The role of a mutant CCR5 allele in
607 HIV-1 transmission and disease progression. *Nat. Med.* 2, 1240–1243.
608 <https://doi.org/10.1038/nm1196-1240>.
- 609 22. Kohn, D.B., Bauer, G., Rice, C.R., Rothschild, J.C., Carbonaro, D.A., Valdez, P., Hao, Q. I,
610 Zhou, C., Bahner, I., Kearns, K., et al. (1999). A clinical trial of retroviral-mediated transfer
611 of a rev-responsive element decoy gene into CD34(+) cells from the bone marrow of human
612 immunodeficiency virus-1-infected children. *Blood* 94, 368–371.
- 613 23. DiGiusto, D.L., Krishnan, A., Li, L., Li, H., Li, S., Rao, A., Mi, S., Yam, P., Stinson, S.,
614 Kalos, M., et al. (2010). RNA-based gene therapy for HIV with lentiviral vector-modified
615 CD34(+) cells in patients undergoing transplantation for AIDS-related lymphoma. *Sci.*
616 *Transl. Med.* 2, 36ra43. <https://doi.org/10.1126/scitranslmed.3000931>.

- 617 24. Yu, S., Ou, Y., Xiao, H., Li, J., Adah, D., Liu, S., Zhao, S., Qin, L., Yao, Y., and Chen, X.
618 (2020). Experimental Treatment of SIV-Infected Macaques via Autograft of CCR5-
619 Disrupted Hematopoietic Stem and Progenitor Cells. *Mol. Ther. Methods Clin. Dev.* *17*,
620 520–531. <https://doi.org/10.1016/j.omtm.2020.03.004>.
- 621 25. Mitsuyasu, R.T., Merigan, T.C., Carr, A., Zack, J.A., Winters, M.A., Workman, C., Bloch,
622 M., Lalezari, J., Becker, S., Thornton, L., et al. (2009). Phase 2 gene therapy trial of an anti-
623 HIV ribozyme in autologous CD34+ cells. *Nat. Med.* *15*, 285–292.
624 <https://doi.org/10.1038/nm.1932>.
- 625 26. Peterson, C.W., Younan, P., Jerome, K.R., and Kiem, H.-P. (2013). Combinatorial anti-HIV
626 gene therapy: using a multipronged approach to reach beyond HAART. *Gene Ther.* *20*, 695–
627 702. <https://doi.org/10.1038/gt.2012.98>.
- 628 27. Holder, K.A., and Grant, M.D. (2020). TIGIT Blockade: A Multipronged Approach to
629 Target the HIV Reservoir. *Front. Cell. Infect. Microbiol.* *10*, 175.
630 <https://doi.org/10.3389/fcimb.2020.00175>.
- 631 28. Qin, X.-F., An, D.S., Chen, I.S.Y., and Baltimore, D. (2003). Inhibiting HIV-1 infection in
632 human T cells by lentiviral-mediated delivery of small interfering RNA against CCR5. *Proc.*
633 *Natl. Acad. Sci. U. S. A.* *100*, 183–188. <https://doi.org/10.1073/pnas.232688199>.
- 634 29. Shimizu, S., Kamata, M., Kittipongdaja, P., Chen, K.N., Kim, S., Pang, S., Boyer, J., Qin,
635 F.X.-F., An, D.S., and Chen, I.S. (2009). Characterization of a potent non-cytotoxic shRNA
636 directed to the HIV-1 co-receptor CCR5. *Genet. Vaccines Ther.* *7*, 8.
637 <https://doi.org/10.1186/1479-0556-7-8>.
- 638 30. Burke, B.P., Levin, B.R., Zhang, J., Sahakyan, A., Boyer, J., Carroll, M.V., Colón, J.C.,
639 Keech, N., Rezek, V., Bristol, G., et al. (2015). Engineering Cellular Resistance to HIV-1

- 640 Infection In Vivo Using a Dual Therapeutic Lentiviral Vector. *Mol. Ther. Nucleic Acids* *4*,
641 e236. <https://doi.org/10.1038/mtna.2015.10>.
- 642 31. Guo, Q., Zhang, J., Parikh, K., Brinkley, A., Lin, S., Zakarian, C., Pernet, O., Shimizu, S.,
643 Khamaikawin, W., Hacke, K., et al. (2024). In vivo selection of anti-HIV-1 gene-modified
644 human hematopoietic stem/progenitor cells to enhance engraftment and HIV-1 inhibition.
645 *Mol. Ther. J. Am. Soc. Gene Ther.* *32*, 384–394.
646 <https://doi.org/10.1016/j.ymthe.2023.12.007>.
- 647 32. An, D.S., Donahue, R.E., Kamata, M., Poon, B., Metzger, M., Mao, S.-H., Bonifacino, A.,
648 Krouse, A.E., Darlix, J.-L., Baltimore, D., et al. (2007). Stable reduction of CCR5 by RNAi
649 through hematopoietic stem cell transplant in non-human primates. *Proc. Natl. Acad. Sci. U.*
650 *S. A.* *104*, 13110–13115. <https://doi.org/10.1073/pnas.0705474104>.
- 651 33. Wolstein, O., Boyd, M., Millington, M., Impey, H., Boyer, J., Howe, A., Delebecque, F.,
652 Cornetta, K., Rothe, M., Baum, C., et al. (2014). Preclinical safety and efficacy of an anti-
653 HIV-1 lentiviral vector containing a short hairpin RNA to CCR5 and the C46 fusion
654 inhibitor. *Mol. Ther. Methods Clin. Dev.* *1*, 11. <https://doi.org/10.1038/mtm.2013.11>.
- 655 34. Zhen, A., Peterson, C.W., Carrillo, M.A., Reddy, S.S., Youn, C.S., Lam, B.B., Chang, N.Y.,
656 Martin, H.A., Rick, J.W., Kim, J., et al. (2017). Long-term persistence and function of
657 hematopoietic stem cell-derived chimeric antigen receptor T cells in a nonhuman primate
658 model of HIV/AIDS. *PLOS Pathog.* *13*, e1006753.
659 <https://doi.org/10.1371/journal.ppat.1006753>.
- 660 35. Yang, O.O., Tran, A.C., Kalams, S.A., Johnson, R.P., Roberts, M.R., and Walker, B.D.
661 (1997). Lysis of HIV-1-infected cells and inhibition of viral replication by universal receptor
662 T cells. *Proc. Natl. Acad. Sci. U. S. A.* *94*, 11478–11483.

- 663 <https://doi.org/10.1073/pnas.94.21.11478>.
- 664 36. Scholler, J., Brady, T.L., Binder-Scholl, G., Hwang, W.-T., Plesa, G., Hege, K.M., Vogel,
665 A.N., Kalos, M., Riley, J.L., Deeks, S.G., et al. (2012). Decade-long safety and function of
666 retroviral-modified chimeric antigen receptor T cells. *Sci. Transl. Med.* *4*, 132ra53.
667 <https://doi.org/10.1126/scitranslmed.3003761>.
- 668 37. Zhen, A., Carrillo, M.A., Mu, W., Rezek, V., Martin, H., Hamid, P., Chen, I.S.Y., Yang,
669 O.O., Zack, J.A., and Kitchen, S.G. (2021). Robust CAR-T memory formation and function
670 via hematopoietic stem cell delivery. *PLOS Pathog.* *17*, e1009404.
671 <https://doi.org/10.1371/journal.ppat.1009404>.
- 672 38. Zhen, A., Kamata, M., Rezek, V., Rick, J., Levin, B., Kasparian, S., Chen, I.S., Yang, O.O.,
673 Zack, J.A., and Kitchen, S.G. (2015). HIV-specific Immunity Derived From Chimeric
674 Antigen Receptor-engineered Stem Cells. *Mol. Ther. J. Am. Soc. Gene Ther.* *23*, 1358–1367.
675 <https://doi.org/10.1038/mt.2015.102>.
- 676 39. Juluri, K.R., Wu, Q.V., Voutsinas, J., Hou, J., Hirayama, A.V., Mullane, E., Miles, N.,
677 Maloney, D.G., Turtle, C.J., Bar, M., et al. (2022). Severe cytokine release syndrome is
678 associated with hematologic toxicity following CD19 CAR T-cell therapy. *Blood Adv.* *6*,
679 2055–2068. <https://doi.org/10.1182/bloodadvances.2020004142>.
- 680 40. Hill, J.A., Li, D., Hay, K.A., Green, M.L., Cherian, S., Chen, X., Riddell, S.R., Maloney,
681 D.G., Boeckh, M., and Turtle, C.J. (2018). Infectious complications of CD19-targeted
682 chimeric antigen receptor-modified T-cell immunotherapy. *Blood* *131*, 121–130.
683 <https://doi.org/10.1182/blood-2017-07-793760>.
- 684 41. Turtle, C.J., Hanafi, L.-A., Berger, C., Gooley, T.A., Cherian, S., Hudecek, M.,
685 Sommermeyer, D., Melville, K., Pender, B., Budiarto, T.M., et al. (2016). CD19 CAR-T

- 686 cells of defined CD4⁺:CD8⁺ composition in adult B cell ALL patients. *J. Clin. Invest.* *126*,
687 2123–2138. <https://doi.org/10.1172/JCI85309>.
- 688 42. Wang, X., Chang, W.-C., Wong, C.W., Colcher, D., Sherman, M., Ostberg, J.R., Forman,
689 S.J., Riddell, S.R., and Jensen, M.C. (2011). A transgene-encoded cell surface polypeptide
690 for selection, in vivo tracking, and ablation of engineered cells. *Blood* *118*, 1255–1263.
691 <https://doi.org/10.1182/blood-2011-02-337360>.
- 692 43. Kao, R.L., Truscott, L.C., Chiou, T.-T., Tsai, W., Wu, A.M., and De Oliveira, S.N. (2019). A
693 Cetuximab-Mediated Suicide System in Chimeric Antigen Receptor-Modified
694 Hematopoietic Stem Cells for Cancer Therapy. *Hum. Gene Ther.* *30*, 413–428.
695 <https://doi.org/10.1089/hum.2018.180>.
- 696 44. Lan, P., Tonomura, N., Shimizu, A., Wang, S., and Yang, Y.-G. (2006). Reconstitution of a
697 functional human immune system in immunodeficient mice through combined human fetal
698 thymus/liver and CD34⁺ cell transplantation. *Blood* *108*, 487–492.
699 <https://doi.org/10.1182/blood-2005-11-4388>.
- 700 45. Smith, D.J., Lin, L.J., Moon, H., Pham, A.T., Wang, X., Liu, S., Ji, S., Rezek, V., Shimizu,
701 S., Ruiz, M., et al. (2016). Propagating Humanized BLT Mice for the Study of Human
702 Immunology and Immunotherapy. *Stem Cells Dev.* *25*, 1863–1873.
703 <https://doi.org/10.1089/scd.2016.0193>.
- 704 46. Ho, J.-Y., Wang, L., Liu, Y., Ba, M., Yang, J., Zhang, X., Chen, D., Lu, P., and Li, J. (2021).
705 Promoter usage regulating the surface density of CAR molecules may modulate the kinetics
706 of CAR-T cells in vivo. *Mol. Ther. Methods Clin. Dev.* *21*, 237–246.
707 <https://doi.org/10.1016/j.omtm.2021.03.007>.
- 708 47. Garcia-Beltran, W.F., Claiborne, D.T., Maldini, C.R., Phelps, M., Vrbanac, V., Karpel, M.E.,

- 709 Krupp, K.L., Power, K.A., Boutwell, C.L., Balazs, A.B., et al. (2021). Innate Immune
710 Reconstitution in Humanized Bone Marrow-Liver-Thymus (HuBLT) Mice Governs
711 Adaptive Cellular Immune Function and Responses to HIV-1 Infection. *Front. Immunol.* *12*,
712 667393. <https://doi.org/10.3389/fimmu.2021.667393>.
- 713 48. Shultz, L.D., Brehm, M.A., Bavari, S., and Greiner, D.L. (2011). Humanized mice as a
714 preclinical tool for infectious disease and biomedical research. *Ann. N. Y. Acad. Sci.* *1245*,
715 50–54. <https://doi.org/10.1111/j.1749-6632.2011.06310.x>.
- 716 49. Schmiedel, J., Blaukat, A., Li, S., Knoechel, T., and Ferguson, K.M. (2008). Matuzumab
717 binding to EGFR prevents the conformational rearrangement required for dimerization.
718 *Cancer Cell* *13*, 365–373. <https://doi.org/10.1016/j.ccr.2008.02.019>.
- 719 50. Mu, W., Patankar, V., Kitchen, S., and Zhen, A. (2024). Examining Chronic Inflammation,
720 Immune Metabolism, and T Cell Dysfunction in HIV Infection. *Viruses* *16*, 219.
721 <https://doi.org/10.3390/v16020219>.
- 722 51. Marsden, M.D., Kovochich, M., Suree, N., Shimizu, S., Mehta, R., Cortado, R., Bristol, G.,
723 An, D.S., and Zack, J.A. (2012). HIV latency in the humanized BLT mouse. *J. Virol.* *86*,
724 339–347. <https://doi.org/10.1128/JVI.06366-11>.
- 725 52. CAR T Cells: Engineering Immune Cells to Treat Cancer - NCI (2013).
726 <https://www.cancer.gov/about-cancer/treatment/research/car-t-cells>.
- 727 53. De Marco, R.C., Monzo, H.J., and Ojala, P.M. (2023). CAR T Cell Therapy: A Versatile
728 Living Drug. *Int. J. Mol. Sci.* *24*, 6300. <https://doi.org/10.3390/ijms24076300>.
- 729 54. Rothemejer, F.H., Lauritsen, N.P., Søggaard, O.S., and Tolstrup, M. (2023). Strategies for
730 enhancing CAR T cell expansion and persistence in HIV infection. *Front. Immunol.* *14*,
731 1253395. <https://doi.org/10.3389/fimmu.2023.1253395>.

- 732 55. Anthony-Gonda, K., Bardhi, A., Ray, A., Flerin, N., Li, M., Chen, W., Ochsenbauer, C.,
733 Kappes, J.C., Krueger, W., Worden, A., et al. (2019). Multi-specific anti-HIV duoCAR-T
734 cells display broad antiviral activity and potent elimination of HIV-infected cells in vivo.
735 *Sci. Transl. Med.* *11*, eaav5685. <https://doi.org/10.1126/scitranslmed.aav5685>.
- 736 56. Hacein-Bey-Abina, S., Von Kalle, C., Schmidt, M., McCormack, M.P., Wulffraat, N.,
737 Leboulch, P., Lim, A., Osborne, C.S., Pawliuk, R., Morillon, E., et al. (2003). LMO2-
738 associated clonal T cell proliferation in two patients after gene therapy for SCID-X1. *Science*
739 *302*, 415–419. <https://doi.org/10.1126/science.1088547>.
- 740 57. Kustikova, O., Fehse, B., Modlich, U., Yang, M., Düllmann, J., Kamino, K., von Neuhoff,
741 N., Schlegelberger, B., Li, Z., and Baum, C. (2005). Clonal dominance of hematopoietic
742 stem cells triggered by retroviral gene marking. *Science* *308*, 1171–1174.
743 <https://doi.org/10.1126/science.1105063>.
- 744 58. Hacein-Bey-Abina, S., von Kalle, C., Schmidt, M., Le Deist, F., Wulffraat, N., McIntyre, E.,
745 Radford, I., Villeval, J.-L., Fraser, C.C., Cavazzana-Calvo, M., et al. (2003). A serious
746 adverse event after successful gene therapy for X-linked severe combined
747 immunodeficiency. *N. Engl. J. Med.* *348*, 255–256.
748 <https://doi.org/10.1056/NEJM200301163480314>.
- 749 59. Dey, D., Evans, G.R.D., Dey, D., and Evans, G.R.D. (2011). Suicide Gene Therapy by
750 Herpes Simplex Virus-1 Thymidine Kinase (HSV-TK). In *Targets in Gene Therapy*
751 (IntechOpen). <https://doi.org/10.5772/18544>.
- 752 60. Di Stasi, A., Tey, S.-K., Dotti, G., Fujita, Y., Kennedy-Nasser, A., Martinez, C., Straathof,
753 K., Liu, E., Durett, A.G., Grilley, B., et al. (2011). Inducible apoptosis as a safety switch for
754 adoptive cell therapy. *N. Engl. J. Med.* *365*, 1673–1683.

- 755 <https://doi.org/10.1056/NEJMoa1106152>.
- 756 61. Griffioen, M., van Egmond, E.H.M., Kester, M.G.D., Willemze, R., Falkenburg, J.H.F., and
757 Heemskerk, M.H.M. (2009). Retroviral transfer of human CD20 as a suicide gene for
758 adoptive T-cell therapy. *Haematologica* 94, 1316–1320.
759 <https://doi.org/10.3324/haematol.2008.001677>.
- 760 62. Dunleavy, K., Tay, K., and Wilson, W.H. (2010). Rituximab-Associated Neutropenia.
761 *Semin. Hematol.* 47, 180–186. <https://doi.org/10.1053/j.seminhematol.2010.01.009>.
- 762 63. Pescovitz, M.D. (2006). Rituximab, an Anti-CD20 Monoclonal Antibody: History and
763 Mechanism of Action. *Am. J. Transplant.* 6, 859–866. [https://doi.org/10.1111/j.1600-](https://doi.org/10.1111/j.1600-6143.2006.01288.x)
764 [6143.2006.01288.x](https://doi.org/10.1111/j.1600-6143.2006.01288.x).
- 765 64. Yoshimoto, K., Murakami, R., Moritani, M., Ohta, M., Iwahana, H., Nakauchi, H., and
766 Itakura, M. (1996). Loss of ganciclovir sensitivity by exclusion of thymidine kinase gene
767 from transplanted proinsulin-producing fibroblasts as a gene therapy model for diabetes.
768 *Gene Ther.* 3, 230–234.
- 769 65. Yang, L., Hwang, R., Chiang, Y., Gordon, E.M., Anderson, W.F., and Parekh, D. (1998).
770 Mechanisms for ganciclovir resistance in gastrointestinal tumor cells transduced with a
771 retroviral vector containing the herpes simplex virus thymidine kinase gene. *Clin. Cancer*
772 *Res. Off. J. Am. Assoc. Cancer Res.* 4, 731–741.
- 773 66. Yanagisawa, N., Satoh, T., Tabata, K., Tsumura, H., Nasu, Y., Watanabe, M., Thompson,
774 T.C., Okayasu, I., Murakumo, Y., Baba, S., et al. (2021). Cytopathic effects and local
775 immune responses in repeated neoadjuvant HSV-tk + ganciclovir gene therapy for prostate
776 cancer. *Asian J. Urol.* 8, 280–288. <https://doi.org/10.1016/j.ajur.2020.06.004>.
- 777 67. Traversari, C., Markt, S., Magnani, Z., Mangia, P., Russo, V., Ciceri, F., Bonini, C., and

- 778 Bordignon, C. (2007). The potential immunogenicity of the TK suicide gene does not
779 prevent full clinical benefit associated with the use of TK-transduced donor lymphocytes in
780 HSCT for hematologic malignancies. *Blood* *109*, 4708–4715. [https://doi.org/10.1182/blood-](https://doi.org/10.1182/blood-2006-04-015230)
781 [2006-04-015230](https://doi.org/10.1182/blood-2006-04-015230).
- 782 68. Gargett, T., and Brown, M.P. (2014). The inducible caspase-9 suicide gene system as a
783 “safety switch” to limit on-target, off-tumor toxicities of chimeric antigen receptor T cells.
784 *Front. Pharmacol.* *5*, 235. <https://doi.org/10.3389/fphar.2014.00235>.
- 785 69. Zhou, X., Stasi, A.D., and Brenner, M.K. (2015). iCaspase 9 Suicide Gene System. *Methods*
786 *Mol. Biol. Clifton NJ* *1317*, 87. https://doi.org/10.1007/978-1-4939-2727-2_6.
- 787 70. Guercio, M., Manni, S., Boffa, I., Caruso, S., Di Cecca, S., Sinibaldi, M., Abbaszadeh, Z.,
788 Camera, A., Ciccone, R., Polito, V.A., et al. (2021). Inclusion of the Inducible Caspase 9
789 Suicide Gene in CAR Construct Increases Safety of CAR.CD19 T Cell Therapy in B-Cell
790 Malignancies. *Front. Immunol.* *12*. <https://doi.org/10.3389/fimmu.2021.755639>.
- 791 71. Gorovits, B., and Koren, E. (2019). Immunogenicity of Chimeric Antigen Receptor T-Cell
792 Therapeutics. *BioDrugs Clin. Immunother. Biopharm. Gene Ther.* *33*, 275–284.
793 <https://doi.org/10.1007/s40259-019-00354-5>.
- 794 72. Lu, L., Xie, M., Yang, B., Zhao, W., and Cao, J. (2024). Enhancing the safety of CAR-T cell
795 therapy: Synthetic genetic switch for spatiotemporal control. *Sci. Adv.* *10*, eadj6251.
796 <https://doi.org/10.1126/sciadv.adj6251>.
- 797 73. Stavrou, M., Philip, B., Traynor-White, C., Davis, C.G., Onuoha, S., Cordoba, S., Thomas,
798 S., and Pule, M. (2018). A Rapamycin-Activated Caspase 9-Based Suicide Gene. *Mol. Ther.*
799 *26*, 1266–1276. <https://doi.org/10.1016/j.ymthe.2018.03.001>.
- 800 74. Shimizu, S., Ringpis, G.-E., Marsden, M.D., Cortado, R.V., Wilhalme, H.M., Elashoff, D.,

- 801 Zack, J.A., Chen, I.S. Y., and An, D.S. (2015). RNAi-Mediated CCR5 Knockdown Provides
802 HIV-1 Resistance to Memory T Cells in Humanized BLT Mice. *Mol. Ther. Nucleic Acids* 4,
803 e227. <https://doi.org/10.1038/mtna.2015.3>.
- 804 75. Ringpis, G.-E.E., Shimizu, S., Arokium, H., Camba-Colón, J., Carroll, M.V., Cortado, R.,
805 Xie, Y., Kim, P.Y., Sahakyan, A., Lowe, E.L., et al. (2012). Engineering HIV-1-Resistant T-
806 Cells from Short-Hairpin RNA-Expressing Hematopoietic Stem/Progenitor Cells in
807 Humanized BLT Mice. *PLOS ONE* 7, e53492.
808 <https://doi.org/10.1371/journal.pone.0053492>.
- 809 76. Shimizu, S., Hong, P., Arumugam, B., Pokomo, L., Boyer, J., Koizumi, N., Kittipongdaja,
810 P., Chen, A., Bristol, G., Galic, Z., et al. (2010). A highly efficient short hairpin RNA
811 potently down-regulates CCR5 expression in systemic lymphoid organs in the hu-BLT
812 mouse model. *Blood* 115, 1534–1544. <https://doi.org/10.1182/blood-2009-04-215855>.
- 813 77. Lee, W.S., Richard, J., Lichtfuss, M., Smith, A.B., Park, J., Courter, J.R., Melillo, B.N.,
814 Sodroski, J.G., Kaufmann, D.E., Finzi, A., et al. (2016). Antibody-Dependent Cellular
815 Cytotoxicity against Reactivated HIV-1-Infected Cells. *J. Virol.* 90, 2021–2030.
816 <https://doi.org/10.1128/JVI.02717-15>.
- 817 78. Telwatte, S., Morón-López, S., Aran, D., Kim, P., Hsieh, C., Joshi, S., Montano, M., Greene,
818 W.C., Butte, A.J., Wong, J.K., et al. (2019). Heterogeneity in HIV and cellular transcription
819 profiles in cell line models of latent and productive infection: implications for HIV latency.
820 *Retrovirology* 16, 32. <https://doi.org/10.1186/s12977-019-0494-x>.
- 821 79. Sarma, N.J., Takeda, A., and Yaseen, N.R. (2010). Colony Forming Cell (CFC) Assay for
822 Human Hematopoietic Cells. *J. Vis. Exp. JoVE*, 2195. <https://doi.org/10.3791/2195>.
- 823 80. Abeynaike, S.A., Huynh, T.R., Mehmood, A., Kim, T., Frank, K., Gao, K., Zalfa, C.,

824 Gandarilla, A., Shultz, L., and Paust, S. (2023). Human Hematopoietic Stem Cell Engrafted
825 IL-15 Transgenic NSG Mice Support Robust NK Cell Responses and Sustained HIV-1
826 Infection. *Viruses* 15, 365. <https://doi.org/10.3390/v15020365>.

827

828 **Figure Legend**

829 **Figure 1. Development of a multi-pronged anti-HIV-1 lentiviral vector with safety kill** 830 **switch to defend against and attack HIV-1 infection**

831 (A) Design of novel lentiviral vectors expressing triple anti-HIV-1 genes (CCR5sh1005,
832 D1D2CAR 4-1BB, C46) and a selectable huEGFRt gene. The M1 vector uses an MNDU
833 promoter and the U1 vector uses a Ubc promoter for D1D2CAR 4-1BB and huEGFRt
834 expression, respectively. These vectors also includes Δ LTR: self-inactivating, U3 enhancer and
835 promoter deleted long terminal repeat, H1: H1 RNA polymerase III promoter, MNDU: murine
836 leukemia virus (MuLV) long terminal repeat promoter, UbC: Ubiquitin C RNA polymerase II
837 promoter, T2A: 2A self-cleaving peptide, huEGFRt: truncated non-functional human epidermal
838 growth factor receptor, EF1 α : human elongation factor 1 alpha promoter, WPRE: woodchuck
839 hepatitis virus posttranscriptional regulatory element. Non-CCR5sh1005 vector includes Δ LTR,
840 MNDU, D1D2CAR 4-1BB, T2A, huEGFRt, C46 and WPRE.

841 (B) Vector titer measured by infectious units/milliliter (IU/ml) determined based on percent
842 huEGFRt transgene expression in 293T cell line stained with CTX-PE mAb and measured by
843 flow cytometry at day 3 post-transduction.

844 (C) CCR5 downregulation by CCR5sh1005 in MT4-CCR5 cell lines. MT4-CCR5 cells were
845 transduced at MOI 1 with vectors M1 and U1. Untransduced and non-CCR5sh1005 vector
846 transduced MT4-CCR5 cells were used as a negative control. 4 days post-vector transduction,

847 CCR5 and huEGFRt were stained with mAbs and measured by flow cytometry. Normalized
848 CCR5 expression within huEGFRt positive population was calculated based on the following
849 formula: ($[\%CCR5+/huEGFRt+population]/([\%CCR5+/huEGFRt+population] + [\%CCR5-$
850 $/huEGFRt+population]) \times 100\%$) and mean fluorescent intensity of CCR5 expression in huEGFRt
851 positive population (MFI) is indicated on the top of representative flow plot.

852 (D) C46 cell surface expression and MFI in MT4-CCR5 cell line at 4 days post-transduction.
853 MT4-CCR5 cells were transduced at MOI 1 with vectors M1 and U1. Mock is untransduced
854 negative control cells. C46 was stained with mAb and measured by flow cytometry.

855 (E) HuEGFRt and D1D2CAR 4-1BB surface protein expression in primary human CD8⁺ T cells
856 4 days post-transduction. CD8⁺ T cells isolated from healthy-donor PBMCs were transduced
857 with M1 and U1 vectors, respectively (MOI 10). Untransduced primary human CD8⁺ T cells
858 were used as a negative control. HuEGFRt and D1D2CAR 4-1BB expression was stained with
859 mAb and measured by flow cytometry.

860 (F) *In-vitro* HIV-1 inhibition by M1 and U1 vector-transduced MT4-CCR5 cells. Untransduced
861 MT4-CCR5 cells were used as a negative control. MT4-CCR5 cells were challenged with R5
862 tropic HIV-1_{NFNSX} (MOI 1) or X4 tropic HIV-1_{NL4-3} (MOI 0.005) virus. p24 capsid protein levels
863 in cell culture supernatant were determined by p24 ELISA assay 7 days post HIV-1 challenge
864 and used to assess inhibition ability. Data shows results from two independent experiments.

865 (G) *In-vitro* specific killing of HIV-1 envelope expressing ACH2 cells. PMA/ionomycin
866 stimulated (Env⁺) or unstimulated (Env⁻) ACH2 cells were co-cultured with vector-transduced
867 human primary CD8⁺ T cells at 1:1, 2:1, and 5:1 Effector:Target cell (E:T) ratio overnight.
868 %specific killing was calculated by ($\%live\ gag+ ACH2\ cells\ with\ untransduced\ CD8+ cell -$
869 $\%live\ gag+ ACH2\ cells\ with\ vector\ transduced\ CD8+ cells$) / $\%live\ gag+ ACH2\ cells\ with$

870 untransduced CD8⁺ cell then normalized by %gag⁺ in ACH2 cells. Data shows Mean \pm SEM
871 from a single experiment performed in triplicates. Mann-Whitney U test was performed to
872 calculate significance. *p <0.05 and **p <0.01.

873

874 **Figure 2. Efficient human HSPC vector-modification, transplantation and multi-lineage**
875 **human hematopoietic cell reconstitution in huBLT mice**

876 (A) Experimental design for the investigation of M1 and U1 vectors in NSG huBLT mice.

877 Human FL-CD34⁺ cells were transduced with M1 or U1 vectors at MOI 3 on Day -1. NSG
878 huBLT mice were conditioned with 270 cGy of sub-lethal body irradiation from a Cesium-137
879 source. Mice were transplanted with the vector transduced FL-CD34⁺ HSPC and human thymus
880 tissue on Day 0. Mice were challenged with R5-tropic HIV-1_{NFNSXSL9} (200ng p24/ mouse) at 11
881 weeks post-transplant.

882 (B) HuEGFRt and D1D2CAR 4-1BB transgene expression in vector transduced FL-CD34⁺ cells
883 in *ex-vivo* culture. HuEGFRt and D1D2CAR 4-1BB co-expressing population was determined by
884 mAb staining and flow cytometry 4 days post-vector transduction.

885 (C) Human multilineage hematopoietic cell reconstitution in peripheral blood from 8 weeks post-
886 vector transduced HSPC transplant. Cell surface markers of human lymphocytes (CD45), T-cells
887 (CD3, CD4, and CD8) and B-cells (CD19) were determined by mAb staining and flow
888 cytometry. Dots and error bars show Mean \pm S.E.M, respectively.

889 (D) Vector-marking levels were determined in peripheral blood cells from 8 weeks to 17 weeks
890 post-transplant by digital PCR. Average vector DNA copies were calculated by $VCN = (WPRE$
891 $DNA \text{ copies in vector DNA}/ul)/(human \beta\text{-globin copies}/ul/2)$. Dots and error bars show Mean \pm
892 S.E.M, respectively.

893 (E) Human multilineage hematopoietic cell expansion within huEGFRt expressing population
894 after HIV-1 infection. Expression of huEGFRt was determined by mAb staining and flow
895 cytometry. Cell surface markers of human lymphocytes (CD45), T-cells (CD3, CD4, and CD8)
896 and B-cells (CD19) were also determined by mAb staining and flow cytometry and gated within
897 the huEGFRt positive population. Mice were challenged with HIV-1 at 11 weeks-post transplant
898 (not noted in this figure). Dots and error bars show Mean \pm S.E.M, respectively. Mann-Whitney
899 U test was performed to calculate significance, * $p < 0.05$.

900 (F) *Ex vivo* cytokine production measured by cytokine release assay. CD8⁺ T splenocytes from
901 M1 huBLT mice were co-cultured with Env⁺ target cells (PMA/ionomycin activated ACH2
902 cells) or unstimulated Env⁻ cells (medium only) as a negative control *ex vivo*. Data was collected
903 from our replicate huBLT mice experiment (donor 2). Cells were collected at time of mouse
904 sacrifice at week 20 post-transplant. Cytokine expression was measured by flow cytometry. Dots
905 and error bars show Mean \pm S.E.M, respectively. *t*-test with Holm-Šídák adjustment was
906 performed to calculate significance. * $p < 0.05$.

907 (G) Viral loads were measured as HIV-1 RNA copies per mL in mouse plasma every 2 weeks
908 post- HIV-1 challenge by digital PCR in 2 different sets of experiments using 2 human CD34⁺
909 HSPC donors (Donor 1 and Donor 2). HuBLT mice groups were transplanted with either M1- (n
910 = 5 in both experiments) or U1-transduced (n = 7) HSPC. Untransduced huBLT mice were used
911 as a negative control in both experiments (n = 3 in first experiment, and n = 5 in replicate
912 experiment). Data were shown in Mean \pm S.E.M. *t*-test with Holm-Šídák adjustment was
913 performed to calculate significance. NS = not significant, * $p < 0.05$, and *** $p < 0.001$.

914

915 **Figure 3. Cetuximab-mediated negative selection of huEGFRt expressing vector-modified**
916 **human hematopoietic cells in huBLT mice**

917 (A) Experimental design for the investigation of CTX-mediated negative selection of huEGFRt+
918 vector-modified human cells. CTX treatment group M1 huBLT mice (n=5) were injected with
919 1mg per mouse intraperitoneally for 11 consecutive days. 5×10^6 human natural killer (NK) cells
920 per mouse were injected retro-orbitally (RO) one day before first treatment (D0) and on D7
921 during CTX treatment. IL-15 expressing lentiviral vectors (2.5×10^6 IU) were injected RO on day
922 7 of CTX treatment (2.5×10^5 IU/mouse). CTX untreated group (n=4) served as a negative
923 control.

924 (B) HuEGFRt expression level in multilineage human peripheral blood cells (CD45+, CD3+,
925 CD19+, CD4+, and CD8+) in CTX treated and untreated M1 huBLT mice. Blood was collected
926 1 week before CTX treatment, and 1 and 4 weeks post-onset of CTX treatment. Samples were
927 stained with mAbs and measured by flow cytometry. HuEGFRt expression was measured by
928 flow cytometry using mAb CTX-PE. Dots and error bars show Mean \pm S.E.M, respectively.
929 Mann-Whitney U test was performed to calculate significance. NS = not significant, and **p
930 <0.01.

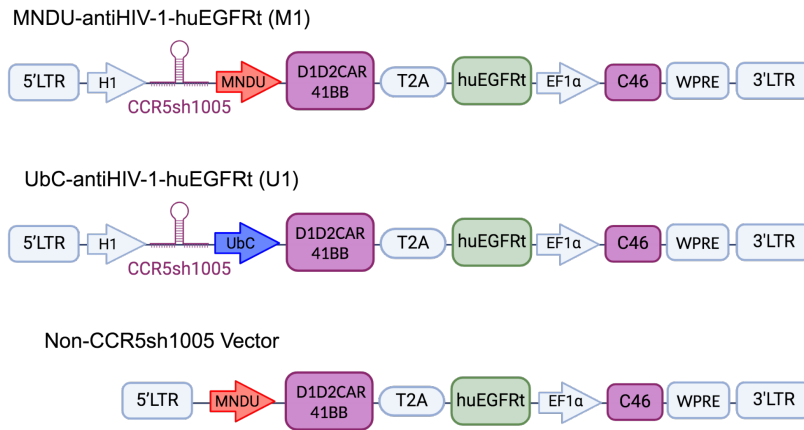
931 (C) Absolute multilineage huEGFRt+ cell count in CTX-treated and untreated M1 huBLT mice
932 in peripheral blood. Blood was collected at weeks 13, 15, and 18 post-transplantation (1 week
933 pre-CTX treatment, and 1 and 4 weeks post-CTX treatment, respectively). HuEGFRt and surface
934 markers of human lymphocytes (CD45), T-cells (CD3, CD4, and CD8) and B-cells (CD19),
935 were stained by mAbs and measured by flow cytometry. Mann-Whitney U test was performed to
936 calculate significance. NS = not significant, *p <0.05, **p <0.01, and ***p <0.001.

937 (D) HuEGFRt expression level across multilineage human T-cell cell populations (CD45+,
938 CD3+, CD4+, CD8+, and CD4+CD8+) in spleen and bone marrow tissue collected from CTX
939 treated and untreated M1 huBLT mice. Samples were stained with mAb CTX-PE. Dots and error
940 bars show Mean \pm S.E.M, respectively. *t*-test with Holm-Šídák adjustment was performed to
941 calculate significance. ***p* <0.01, ****p* <0.001 and *****p* <0.0001.

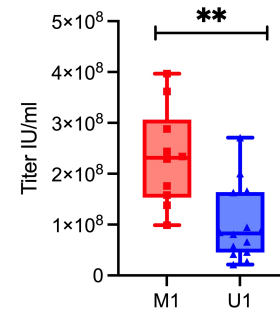
942 (E) Representative flow cytometry data showing huEGFRt expression within
943 CD34+/CD90+/CD38- population of bone marrow cells in CTX treated and untreated M1
944 huBLT mice. Samples were stained with mAb CTX-PE and measured by flow cytometry.

945 (F) Cumulative data showing huEGFRt expression within CD34+/CD90+/CD38- population of
946 bone marrow cells collected from CTX treated and untreated M1 huBLT mice. Samples were
947 stained with mAb CTX-PE and measured by flow cytometry. % huEGFRt was normalized to
948 background levels from mock transduced HSPC transplanted huBLT mice. Dots and error bars
949 show Mean \pm S.E.M, respectively. Student's *t*-test was performed to calculate significance. **p*
950 <0.05.

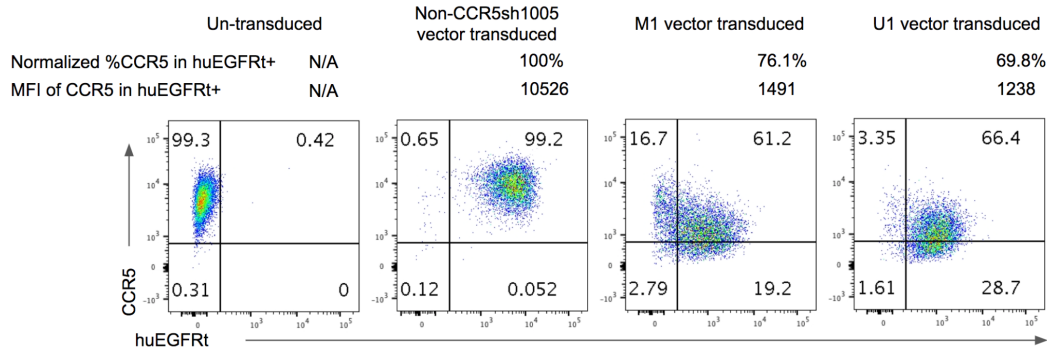
A



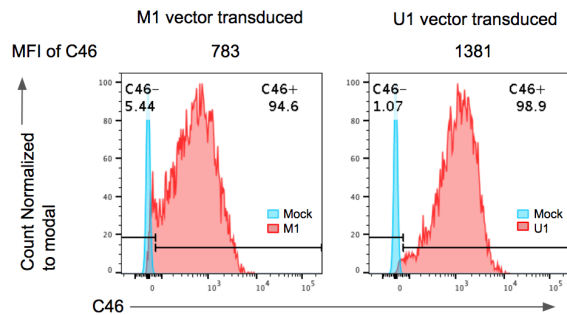
B



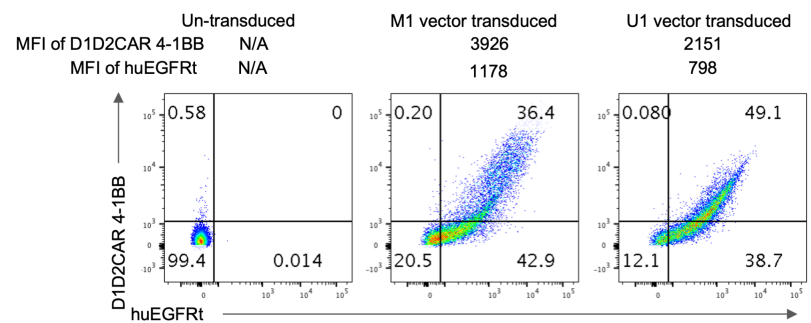
C



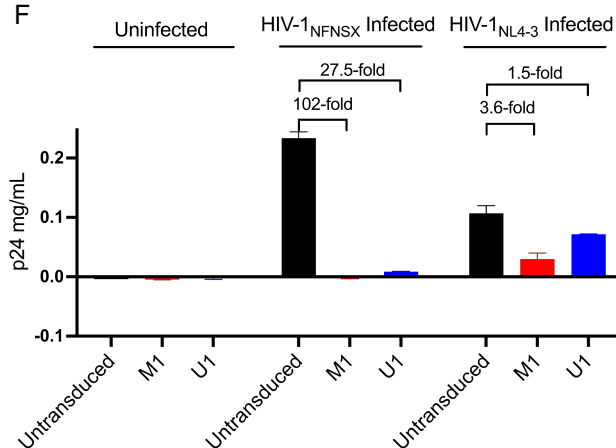
D



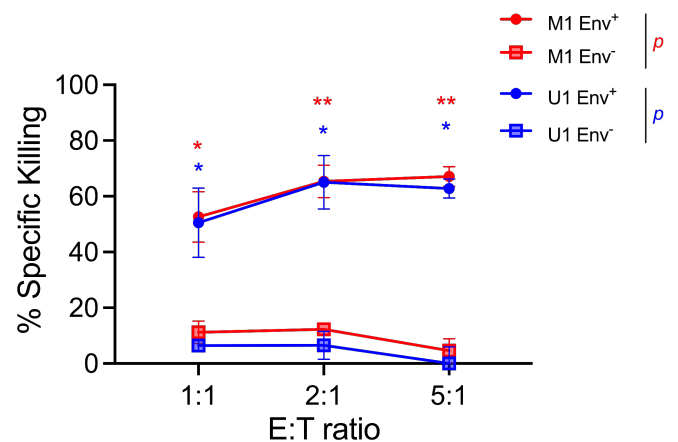
E

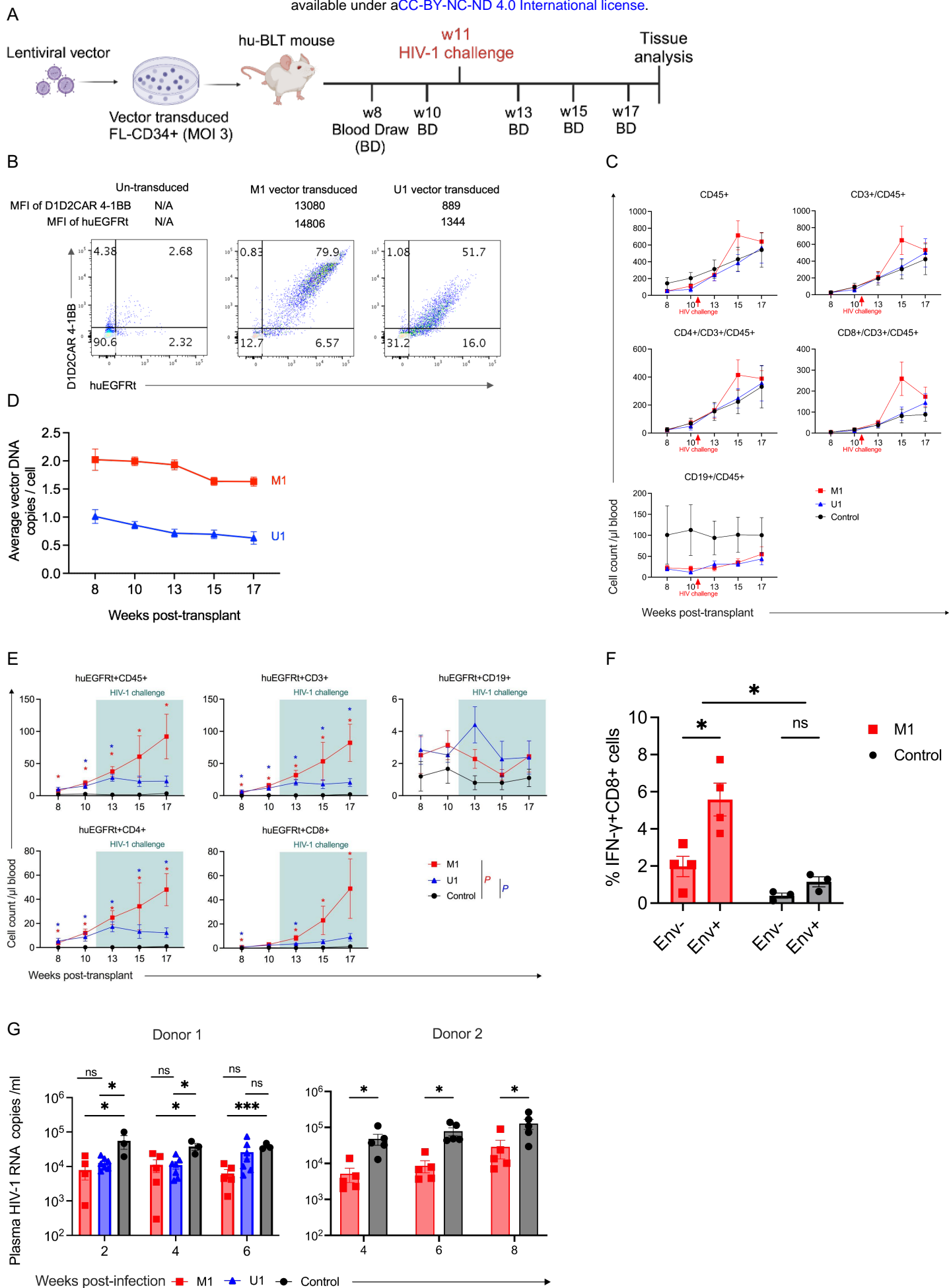


F

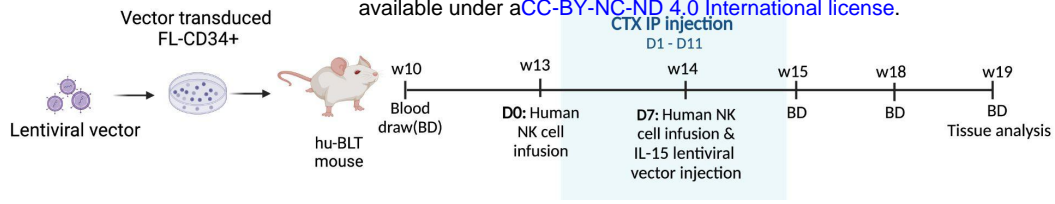


G

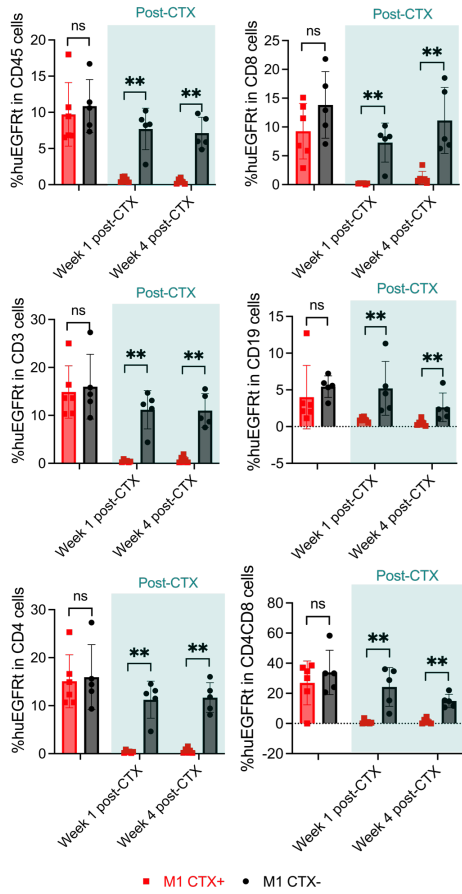




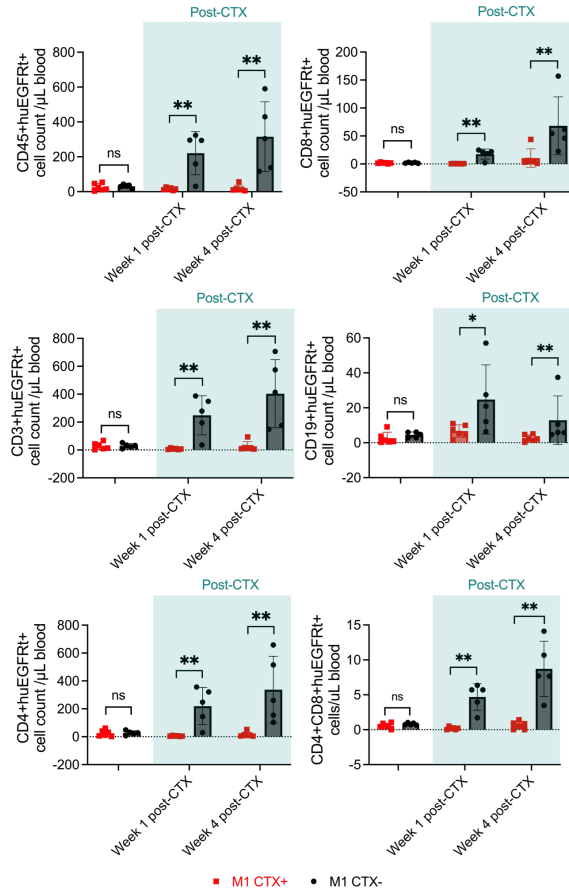
A



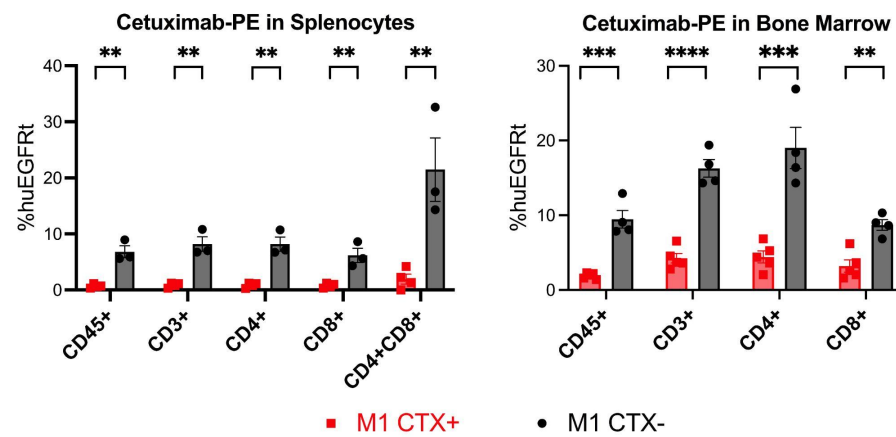
B



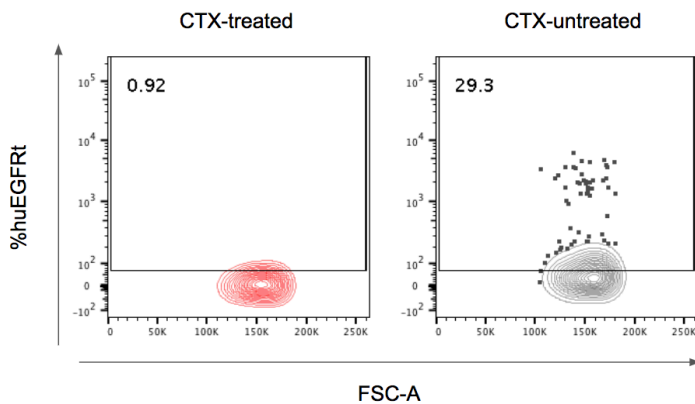
C



D



E



F

